Characterization of expanded polystyrene (EPS) blocks under cyclic pavement foundation loading

S.M.A. Ghotbi Siabil[1], S.N. Moghaddas Tafreshi[2*], A.R. Dawson[3], M. Parvizi Omran[4]

[1]PhD Candidate, Department of Civil Engineering, K.N. Toosi University of Technology, Valiasr St., Mirdamad Cr., Tehran, Iran. Tel: +982188779473; Fax: +982188779476; E-mail address: aminghotbi@gmail.com

[2,]Corresponding Author. Professor, Department of Civil Engineering, K.N. Toosi University of Technology, Valiasr St., Mirdamad Cr., Tehran, Iran. Tel: +982188779473; Fax: +982188779476; E-mail address: nas_moghaddas@kntu.ac.ir*

[3]Associate Professor, Nottingham Transportation Engineering Centre, University of Nottingham, Nottingham, UK. Tel: +441159513902; Fax: +441159513909; E-mail address: andrew.dawson@nottingham.ac.uk

[4]MS. Graduated, Department of Civil Engineering, K.N. Toosi University of Technology, Valiasr St., Mirdamad Cr., Tehran, Iran. Tel: +982188779473; Fax: +982188779476; E-mail address: milad.parvizi.omran@gmail.com

Abstract

This study introduces a mechanism for initial assessment and further development to improve understanding of EPS behavior as a super-lightweight material for road construction. Large scale cyclic plate load tests on model pavements were performed. The effect of several factors including thickness of soil, thickness of subsequent EPS layers and density of EPS on the surface deformations, resilient modulus (M_r) and interlayer pressure transfer were investigated. The results indicated that compared to a covering soil layer of 300 mm, the rut depth on the loading surface reduced by 13.5% and 40.8% when the soil thickness was increased by 33% and 100%, respectively. With a constant soil thickness, increasing the thickness of an upper (denser) EPS layer with respect to a bottom (softer) EPS layer, from 200 mm to 600 mm, would only result in a 20% decrease in the peak settlements at the loading. Resilient modulus of the system was found to be dependent on soil thickness and a designer can choose an appropriate resilient modulus assuming the soil-EPS composite acts as subgrade or subbase. In order to extend the results to a wider range of geofoams, soils and layer thicknesses, a simple stress analysis method was also trialed.

Keywords: *geosynthetics, EPS geofoam, cyclic plate load tests, pavements, lightweight fill*

1 Introduction

In recent years, various methods and materials have been implemented for improvement of pavements subjected to cyclic traffic loading. A major part of these studies utilize previously well-known pavement evaluative methods such as cyclic plate loading tests, while several attempts have also made to introduce more novel methods. From another perspective, some studies have focused on assessment of sustainable and recycled material, while others simply investigated conventional materials using the new assessment techniques (Gnanendran et al. 2011; Piratheepan et al. 2012; Arulrajah et al. 2013; Arulrajah et al. 2014; Rahman et al. 2015; Donrak et al. 2016; Piratheepan et al. 2016; Arulrajah et al. 2017; Georgees et al. 2018; Tavira et al. 2018). Piratheepan et al. (2012) introduced a combined method from the Indirect Diametral Tensile (IDT) and Unconfined Compressive Strength (UCS) tests to determine cohesion and internal friction angle of a pavement's granular material stabilized with slag lime and general blend (GB) cement-fly ash. Tavira et al. (2018) conducted laboratory tests and field investigations including plate load and falling weight deflectometer tests to assess mechanical properties of construction and demolition waste (CDW) in the form of non-selected mixed recycled aggregates as base and subbase bound materials.

While sustainability considerations are of prime importance nowadays, there are circumstances where maximum possible reduction in the weight of material becomes a priority. Recent examples of these situations are reported by Özer & Akınay (2019), Duškov et al. (2019) and Vaslestad et al. (2019). In such cases, EPS geofoam has been introduced as a super lightweight cellular geosynthetic material comprising several advantageous characteristics for application in geotechnical and highway engineering. It has been used successfully in a variety of projects including backfill for retaining walls, bridge abutments and as subgrade for roads and highways worldwide (Stark et al., 2012; Bartlett et al., 2015). In the past 40 years, many countries including, but not limited to, Norway, Sweden, USA, Japan and Turkey have befitted from ultra-light weight of EPS in a variety of projects. As the unit weight of EPS geofoam ranges around a typical value of 1% of a conventional soil's unit weight, it helps to reduce dead load, as well as seismic loads, on structures. It can be handled easily and quickly compared to common construction materials (e.g. soil). These attributes greatly assist in speeding up the rate of construction and delivering projects much faster and, therefore, increasing the economic efficiency of the project. Besides these benefits, EPS also contributes to a lighter design of nearby structures (retaining walls, culverts etc.) because of a very low Poisson's ratio and its energy dissipation characteristics (due to its very low density).

Despite these benefits, there has been a few failure events (excessive settlement, rutting etc.) related to improper usage or design of an EPS system in a highway – where the misunderstanding about the behavior of

EPS in that application was determined to be the main reason. On the other hand, application of EPS geofoam in construction practice is rising continuously, as its valuable features are becoming evident more than ever. However, a true cost-effective approach with respect to real behavior of EPS in actual conditions is nearly neglected by existing guidelines (e.g. in Stark et al., 2004). As the required volume of EPS for highway construction is very high, reducing the density of EPS even if it is a minor reduction, contributes to a huge reduction in the overall cost of the project. The above discussion suggests that implementation of EPS geofoam should be done with more consideration and further research is postulated regarding a safe and efficient design.

Several researches on EPS geofoam application in geotechnical projects such as road construction, buried pipe and culvert protection, retaining walls, etc. have been conducted (Duskov, 1997; Zou et al., 2000; Negussey, 2007; Farnsworth et al., 2008; Barrett and Valsangkar, 2009; Kim et al., 2010; Horvath, 2010; Stark et al., 2012; Tanyu et al., 2013; Anil et al., 2015; Bartlett et al., 2015; Keller, 2016; Witthoeft and Kim, 2016; Ozer, 2016; Beju and Mandal, 2017; Meguid et al., 2017a,b; Gao et al., 2017a,b; Shafikhani et al., 2017; AbdelSalam and Azzam, 2017; Mohajerani et al., 2017; Pu et al., 2018). To figure out the background of research with a special focus on road and highway embankments, the following summary is presented.

Duskov (1997) has illustrated strain and deflection measurements of a constructed road on EPS subgrade in Rotterdam. The subgrade consisted of 1 m thick EPS blocks subjected to heavy traffic loads. He explained that inappropriate pavement design and use of over-estimated E-values for road-base materials led to an inability of EPS to provide proper support for road-base materials. Measurements also revealed that open joints or gaps between EPS blocks significantly reduce the design life of the pavement and must be completely avoided.

However, Zou et al. (2000) discovered that the number of joints between EPS blocks is not the only factor affecting the performance and design life of pavement. They also realized that the performance of EPS subgrade can be as good as sand in terms of plastic deformation under cyclic loading of traffic; and sometime it is more efficient. EPS subgrades tend to generate deeper ruts on the pavement surface compared to sand subgrades with an equal pavement system. They also found out that the size of the EPS blocks and their lateral restraints did have an apparent consequence on the performance of blocks.

Field and laboratory tests by Negussey (2007) has revealed that modulus values of larger EPS blocks are greater than those of smaller ones and the strains measured in small tests can be decreased by up to 50% for real applications. The authors emphasized the need for appropriately assessing the stress redistribution caused by a load distribution slab positioned between a flexible or rigid pavement and geofoam. This must be considered for traffic loading applications.

The I-15 Reconstruction Project is an example of the application of several methods to speed up construction process, while preventing large settlements due to poor ground conditions. A comparative study on the performance of the techniques is presented by Farnsworth et al. (2008). This case history showed that while each of the techniques were suitable for a specific purpose, EPS geofoam was expected to exhibit acceptable post construction settlements for a working period of 50 years.

Horvath (2010) have reported failure modes caused by improper usage or design of EPS in geotechnical applications. According to his report, creep will cause EPS to compress significantly over time (longer than 1000 hours), if it is strained beyond its elastic limit during that time. Negussey (2007) demonstrated, however, that creep is not a definite concern in the field observations, in situations where it had been identified to be critical in preceding tests on smaller samples. Field results indicated that creep strains remained in their initial stages and did not lead to rupture in the pavement. However, the objective of the current study is limited to highways, and such a pattern of loading is very rare in such applications. According to Horvath's (2010) research, the presence or absence of load distribution slabs (LDS) does not have a direct effect on the satisfactory performance of the pavement overlying the EPS. He emphasized that overstressing EPS due to insufficient thickness of soil, and its consequent total and differential settlements, is the key issue in poor performance of the embankment. He has indicated that if existing practices and experiences are properly utilized by designers, such failure would reduce to a minimum amount. An overview of relevant studies is presented in **Table 1**.

Review of this literature indicates that while some large scale laboratory and field studies are indeed available in this area, they have not directly investigated the factors affecting performance, and it is difficult to obtain a quantitative trend for the consequence of each factor. Additionally, there have been obstacles preventing EPS geofoam from becoming a standard worldwide solution as a lightweight fill for pavement. Further investigations are required to boost the technical knowledge, update standards and deliver innovative applications regarding EPS geofoam in pavement construction (Mohajerani et al., 2017). To achieve these goals and find an economic and efficient design process for EPS embankments and to prevent possible future failures, a series of cyclic plate load test were conducted in the study reported here. These tests were organized to help evaluate factors such as variations in thickness of soil and EPS geofoam layers, EPS density and the applied pressure amplitude. The results helped to determine the trend of response to influential parameters and to find their optimum values.

2 Objectives

Failures in pavements including EPS geofoam might have led to many designers avoiding its application despite the great features it can provide (Horvath, 2010). Hence, similar to other novel methods, evaluation of unknown (or less known) aspects of designing and building EPS geofoam subgrades seems to be essential. This has created a motivation for the current study with the aim of producing a better understanding and elimination of current shortcomings.

Therefore, a number of large-scale tests were accomplished to find out the exact behavior of EPS blocks, soil and the full road section comprised of soil layer over several layers of EPS block under application of cyclic loading. Sample sized tests on cubic EPS geofoam blocks by uniaxial cyclic and static test were also conducted to characterize the behavior of EPS geofoam. A summary of the key objectives of the main experimental program using large scale model can be described as:

- Exploration of performance of EPS embankments compared with soil embankments,
- Evaluation of pressure distribution with depth of EPS embankments,
- Assessment of effects of cyclic loading intensity, soil and upper EPS layer thickness, EPS density (stiffness) and thickness of EPS block layers on surface settlement, resilient modulus and transferred pressure on EPS geofoam blocks.

3 Materials

3.1 Soil

The soil used as the upper layer and protective cover over EPS layers was supplied from a quarry near Tehran. Three classes of soil including sand and gravel were brought and mixed, proportionally by weight, to attain the grading diagram shown in **Fig. 1**. This blend of aggregates was classified as a well-graded sand (SW) based on the specifications of the Unified Soil Classification System (ASTM D 2487-09). According to ASTM D 2940-09, this soil is appropriate for use in base and subbase of highways and airports.

Compaction to the Modified Proctor standard, which is widely used as the reference density to which in-situ compaction is benchmarked, showed that this soil can gain a maximum dry density of 20.42 kN/m^3 (ASTM D 1557-12) at about 5% optimum water content. The soil had a specific gravity (G_s) equal to 2.66 with maximum and mean grain size of 20 mm and 4.3 mm, respectively. Using triaxial compression tests on specimens of soil at a wet unit weight of 19.72 kN/m^3 (equivalent to about 97% of the Modified Proctor maximum density) and a moisture content of 5%, the internal friction angle of soil was found to be 40.5º. Further information regarding the soil grading is available on **Fig. 1**.

3.2 EPS geofoam

EPS blocks were supplied from a regional molder in Iran. The original block size was 2000×1000×1000 m and it was cut into desired dimensions (1000×500 mm in plan and 100 or 200 mm in height) by using hot wire cutters. The test method for characterization (e.g. EPS density, compressive strength and elastic modulus) and selection of EPS material were in accordance with the requirements provided in ASTM D 6817-04, ASTM D 1621-00. Unconfined static and cyclic tests on EPS samples were also performed according to ASTM D 1622-08 and a detailed discussion on their results for densities of 20, 30 and 40 kg/m^3 is provided in Section 6.1. A summary of the engineering properties of EPS is shown in **Table 2**. This EPS geofoam is comparable to those used in other research (e.g. Stark et al., 2004) in terms of variation of compressive strength with EPS density, which will be further discussed in Section 6.1.1. Nevertheless, the properties are presented and one can choose a close match with those they might use.

3.3 Geotextile

According to recommendations of previous studies (e.g. Stark et al., 2004), a geotextile layer has to be used as a separator between soil and EPS geofoam blocks to prevent possible damage to EPS layer. Thus, a non-woven geotextile with the typical characteristics as **Error! Reference source not found.** was used. This geotextile is a needle-punched and heat-bonded, being made of UV-stabilized polypropylene. It can be used in building and construction applications for separation, filtration, reinforcement and protection.

4 Test components and layout

The large scale plate load tests, simulating real conditions, were performed in a test box, excavated inside the "Research Laboratory of Physical Modeling in Geotechnics" at the K.N. Toosi University of Technology. In the current study, the model tests comprise a test box, reaction frames, loading system and measurement equipment (see the schematic view in **Fig. 2**).

4.1 Test box and simulated loading

The test box was 1200 mm in depth and 2200×2200 mm in plan (see **Fig. 2**), with the walls and bottom covered with a rough mixture of cement-sand mortar. In the majority of tests, the failure mechanisms have been observed to be of a similar punching nature and the failure surface does not extend, laterally, to a distance further than 3-4 times of loading plate diameter from the center of loading (i.e. a diameter ≤1.2m). As a confirmation to this observation, Moghaddas Tafreshi et al. (2014) reported that, if the horizontal plane dimensions of the test box are equal to seven times of the diameter of the loading surface, that would be enough to prevent the effect of side boundaries. These tests are similar to the tests including soil layer over EPS block layers. According to the results from preliminary experiments (see Section 6.2.3), the depth of the box seems to be sufficient. Measurements indicated that the amplitude of pressure transferred to depths below 1000 mm are equal to a negligible portion of the applied stress on the top of embankment (Section 6.2.3). Therefore, the probable rigid boundary effect initiating from the bottom of the test box is insignificant. Tests by Moghaddas Tafreshi et al. (2012) also showed that a minor portion of applied tire pressure on the soil surface will penetrate to levels deeper than 700 mm. Thus, the box dimensions are suitable for avoidance of boundary influences. For this reason, 1200 mm height of the soil was considered to be adequate in order to reduce boundary effect at the bottom of the test box.

The loading frame consisted of a heavy reaction beam, supported on two strong columns (see **Fig. 2**). A hydraulic jack with capacity of 100 kN and capable of producing monotonic and cyclic movements was fixed above the reaction beam. The loading was applied to a rigid steel plate of 300 mm diameter and thickness of 25 mm on the pavement surface through adjustable rigid steel shafts. The rigid steel plate is representative of the tire of a common truck and exerts the load from hydraulic jack to the surface of the pavement. Regular traffic loading will hardly be applied to the upper soil and EPS layers, although millions of cycles of such load will be applied by such traffic to the overlying asphalt layers. Such loading will be applied for a few traffic passages during construction and this will, likely, be the most demanding time for the pavement studied here. In addition, AASHTO T 221-90 and ASTM D D1195-09 both allow application of a few plate load cycles so as to evaluate airport and highway pavements. Several previous studies including Thakur et al. (2012), have also applied a similar number of load cycles (or even less) for this purpose. To simulate the critical loading that might be applied to a road surface, Brito et al. (2009) suggested applying cyclic pressures of 400 and 800 kPa (representative of half and full trucks, respectively). Although, EPS geofoam is rarely used in unpaved roads, Brito's pressure values are impractical in the case EPS embankments (Stark et al., 2004) and, for the present study, must be reduced to allow for the stress distribution that would be provided by the thickness and stiffness of the pavement's asphalt layer. Using KENPAVE software (Huang, 1993) and assuming 50 mm asphaltic layer with Young's Modulus of 2.5 GPa, the pressure amplitudes can be reduced to 275 and 550 kPa respectively to represent the stress passed down to the top of the soil layer.

Although the rate or frequency of loading might have a direct effect on the response of EPS embankments, a wide range of frequencies (e.g. 0.01~10 Hz) have been implemented by previous researchers for this purpose (Palmeira and Antunes; 2010, Yang et al.; 2012, Thakur et al.; 2012 and Gonzalez-Torre et al.; 2015). Gonzalez-Torre et al (2015) concluded that high frequency loading does not affect the pavement significantly and the lower the frequency, the higher impact will the loading have. In this research and because of loading system limitations, a sinusoidal 0.1 Hz cyclic load was applied, which is a reasonable choice, within the limits of the above studies.

In all tests, the lower pressure (275 kPa) was applied 100 times, followed by 400 repetitions of the higher pressure (550 kPa). Although the number of vehicle passes will definitely exceed these values by a large margin, the pressure will be most critical in the construction phase of the road backfill, when the soil thickness is thinnest. At such a stage, 500 axle passages is a reasonable approximation to reality as shown by Powell et al (1984).

4.2 Measurement system

The measurement system of the large scale cyclic plate load test is shown in schematically in **Fig. 2**. Two LVDTs were placed above the rigid plate and the settlements of the loading surface were measured using their average value. To obtain an approximate sketch of the deflection basin in some of the tests, two additional LVDTs were also placed at 100 mm and 150 mm away from the edge of the loading plate in a few tests. The LVDTs had an accuracy of ±0.01% at their full range (75 mm). A S-shaped load cell was placed between hydraulic jack and the rigid plate to control the amplitude of applied load. The capacity of the load cell was 100 kN and its accuracy was ±0.01%. In all of the experiments, an earth pressure cell was placed above the upper layer of EPS geofoam (between soil layer and EPS bed) to read the amplitude of the pressure transferred to the top of the EPS layers. In such type of pavements, the amplitude of pressure transferred on top of EPS layer would have an acute influence on pavements' performance (Shafikhani et al., 2018) and controlling its value is considered an important part of the design procedures (Stark, 2004). The transferred pressure to lower depths was considered negligible and thus, the pressure at deeper levels of EPS bed was only measured in a few tests. It is also worth mentioning that all of the sensors and pressure cell were calibrated using proper calibration method to ensure the accuracy of the recorded data. The sensors were connected to a data logger, and the measured data were sent to a computer, which saves and presents data for future analyses.

4.3 Backfill preparation and test procedure

The initial stage was to fill the test box with EPS geofoam blocks. Zou et al. (2000) found that size and lateral restraints have no significant effect on the performance of geofoam blocks. Making use of this finding, the blocks were ordered to be prepared as 1000×500 mm in plan and 100 or 200 mm in height in order to have flexibility in replacing deformed or damaged blocks with more intact ones, to minimize disposal costs and to provide longer life spans for the current testing material. After each test, the geofoam blocks that were not visibly damaged were used in some location other than directly under the loading plate for the next test to reduce EPS geofoam disposal. A few tests were also repeated by replacing some of the larger EPS blocks but the results did not show a noteworthy difference.

EPS blocks were located at bottom of the test pit with minimum lateral (horizontal) gap between them. Yet a slight gap is unavoidable in most cases, although, it will not affect the overall performance of the section, as reported by Zoe et al. (2000). Adjacent blocks were investigated for any unbalanced vertical alignment or varied surface levels. Any surrounding voids at the corners were also filled and leveled by smaller pieces of EPS. Reaching a perfect surface in terms of surface smoothness and flatness is almost impossible, but maximum effort was made to establish such a condition. Each subsequent layer of EPS was constructed by aligning the length of EPS blocks perpendicular to orientation of their bedding blocks and examined if there was any vertical gap between the blocks due to unleveled seating (Stark et al., 2004).

The selected height of 100 or 200 mm for EPS blocks also helped to examine the effect of EPS density and thickness at the subsequent layers. To this aim, the blocks in each layer were replaced with the desired density and height, so an appropriate order of blocks were formed from top to bottom of the test box (see **Fig. 2**). It is a well-known practice (Stark et al., 2004) to place a layer of higher density EPS as the uppermost layer, in order to control excessive local deformation or failure of EPS, directly below the pressurized zone of overlying soil (Stark et al., 2004), while the major portion of subgrade is constructed with a lower density EPS in order to reduce costs. In other words, a balance has to be established between cost and the maximum allowable rut depth of the pavement surface. This approach was also used in the current study, and the majority of test sections comprised a top layer of EPS with a higher nominal density (e.g. 30 kg/m^3) than the remainder of the EPS (e.g. 20 kg/m^3) as shown in **Fig. 2**. The test box after placement and arrangement of the first layer of EPS blocks is illustrated in **Fig. 3a.**

Observations during the current tests have showed that even a 10~20 mm vertical gap between EPS layers can be extremely destructive and translate into a twofold to threefold increase in the rut depth on the pavement surface, compared to tight placement of the blocks. Therefore, it is important to place EPS blocks with great accuracy to avoid such negative consequences. More details on the requirement on the layout and placement of EPS blocks can be found in ASTM D 7180-05.

No type of connection or adhesion was found to be required between EPS blocks in this study. Barrett and Valsangkar (2009) have reported about the effectiveness of connectors on the shear resistance of geofoam blocks. They performed shear tests on blocks with no connection, blocks with barbed plate connectors and blocks with polyurethane adhesive. They applied different normal pressures on the blocks with each of the connection methods and compared their shear resistance. The results revealed that barbed plates had little influence on the shear resistance between blocks; rather they might impose a slight reduction in the initial shear resistance between the blocks under cyclic loading. However, they did not affect peak shear resistance between the blocks. Polyurethane adhesive could lead to an up to twofold increase in the shear resistance by eliminating horizontal sliding of blocks. Using such adhesives is not a practical approach for real projects and hence was not considered in the current study. Barbed plate connectors were not used either, in order to eliminate their potential destructive effect on the surface of geofoam blocks.

As recommended by Stark et al. (2004), a layer geotextile cover was employed over the final EPS geofoam surface, as a separation and protective method between EPS and soil layer. Soil particles could, potentially, indent the surface and conceivably destroy EPS blocks by eroding EPS particles away from the block. Placement of this geosynthetic layer for high-rise embankments, where using minimum soil thickness is desirable, is essential and helps to increase the longevity of EPS blocks. Thereafter, soil was transferred manually onto the test pit by means of hand shovels, reaching a specified thickness after leveling its surface. A walk-behind vibrating plate compactor of 450 mm width was utilized in order to compact the leveled soil bed. The influence depth of the compacter was between 50 to 100 mm, as reported by the manufacturer. Thus, passage of the compactor over a soil layer with thickness of 100 mm would not have influenced compaction of the bottom layers. To ensure that soil has reached its ultimate state of compaction, each layer was compacted with at least 5 passes of the compactor with the compactive effort kept approximately the same for each layer. **Fig. 3b** shows the completed test installation including reaction beam, loading plate, hydraulic jack, load cell and LVDTs.

In-situ density tests (according to ASTM D 1556-07) and water content tests were performed at random intervals to guarantee the consistency of the soil condition during the experimental program. Water content was maintained close to the optimum water content (5%) with a maximum of 0.25% deviation. Density tests revealed that the maximum achievable dry density (compaction) varied across the vertical profile of the compacted soil, changing from a minimum lower value in the soil layer just above EPS blocks and rising to larger values with increase in soil thickness. Because of the low mass of EPS blocks and their vibrations, the dry density of the first soil layer (adjacent to EPS bed) could not go beyond 18.7 kN/m^3 (equivalent to 92% of maximum compaction). The second and third layer of soil could ultimately reach 19.1 kN/m^3 and 19.4 kN/m^3, respectively. The maximum dry density of the fourth layer and beyond was 19.6 kN/m^3 (96% of maximum compaction). As will be discussed later, this trend is a consequence of the lower stiffness support provided by the EPS.

5 Tests program and parameters

The performance of the pavement was evaluated in terms of depth of ruts generated on the pavement surface and in part, by the transferred pressure to the top of upper EPS layer. To evaluate the effect of the soil layer thickness (h_s) over the EPS layers, the thickness of the upper and bottom EPS layers (h_{gt} and h_{gb}, respectively) and the density of the upper and bottom EPS blocks (γ_{gt} and γ_{gb}, respectively) on the response of EPS backfills, large scale cyclic plate load tests were planned as shown in **Table 4** (where index "g" stands for geofoam and indexes "t" and "b" stand for top and bottom EPS layers, respectively). A total of 19 independent test were performed to achieve the required data for analysis of each factor.

The main repeated plate load tests comprised six series as described in **Table *4***. In Test Series 1, cyclic plate load tests were performed on soil backfill (with no EPS block) with two compactions to determine how density of compacted soil can influence stiffness and settlements. In Test Series 2, the amplitude of applied pressure was varied to discover its effect on the settlements of pavement sections including soil and EPS layers. Test Series 3 was performed to determine how pressure dissipates with depth in the EPS body. As only one pressure cell was available during the experimental program, the pressure sensor had to be placed at depths of 400, 600, 800, 1000 and 1200 mm below the loading surface in separate tests, therefore, Test Series 3 had to be repeated 5 times. In Test Series 4, the effect of soil thickness was investigated. Test Series 5 consisted of experiments to evaluate the influence of the thickness of the upper (denser) EPS layer and finally, Test Series 6 focused on assessing the effect of the upper EPS density on the performance of the pavement.

Regarding the selection of soil thickness and EPS layers in Table 3, further discussion would be useful. The Swedish standard (1987) and the Norwegian standard (1992) recommend a minimum value of 400 mm to 500 mm and 400 to 800 mm for the thickness of pavement system over EPS geofoam blocks, respectively. Stark et al. (2004) have recommended a minimum pavement thickness of 610 mm (including soil layer and asphalt/concrete slab) to be used over EPS blocks. Due to the limitation of the depth of test box in this study, a typical thickness of 400 mm has been used in the tests. Another reason for selecting such a low thickness was so as not to conceal the effect of remaining factors which might, otherwise, have been too small to be readily observed. (Stark et al., 2004) recommended that at least two layers of EPS geofoam with typical thickness of 610 mm to 1000 mm be used to prevent shifting of the blocks under traffic loads. As the thickness of EPS blocks were 200 mm in the current study, 3 to 4 layer of EPS have been used to comply with the recommended number of layers.

In addition to the main large-scale cyclic tests (**Table 4**), a set of small static and cyclic uniaxial tests were also conducted on 200×200×200 mm cubic specimens of EPS with different densities, in accordance with ASTM

D 1621-00. Cubic shape specimens were preferred to a cylindrical shape because it was easier to prepare them with available manual cutting methods. The static tests were performed to measure elastic and plastic limits and the cyclic tests were also performed to evaluate the cyclic response of EPS block. The reason for selecting these cubic sample tests for EPS alone was that testing of EPS geofoam directly by plate load test is not entirely representative of the real condition and might produce incorrect results due to the generation of cracks in the EPS blocks, due to pressure concentration (overstressing) along the edges of the plate.

In order to check the repeatability of the test results, a few tests were repeated in each Test Series to ensure that there was no significant change in the test procedures during the experimental program. A close match between results of the repeated tests with a maximum difference of 4-6% was observed.

6 Results and discussion

Presentation and discussion of the results of tests are illustrated in this section. In the first part (Section 6.1), the result of uniaxial static and cyclic test on cubic EPS samples are discussed and, in Section 6.2, the results of the main cyclic plate load tests are reported. The test results have been presented in terms of peak surface settlement, permanent surface settlement (as an indicator of rut depth) and resilient modulus of the pavements – the first and last of these having implications for the longevity of performance of overlying bound layers that will have to flex repeatedly over the soil-EPS composite.

6.1 Behavior of cubic EPS samples

A thorough understanding of the behavior of EPS per se will provide a great aid to realize the role of EPS in the overall behavior of these pavement systems, and to recognize what happens when EPS blocks are incorporated in conjunction with soil. Previous research is available about the sole behavior of EPS geofoam in static and dynamic/cyclic conditions: Horvath (1994); Duskov (1997), Athanasopoulos et al. (1999), Trandafir et al. (2010), Ossa and Romo (2011), Trandafir et al. (2012) and Bartlett (2015). To evaluate the behavior of EPS geofoam used in the current study, unconfined uniaxial static and cyclic plate load tests were performed on EPS 20, EPS 30 and EPS 40 (abbreviation of EPS block with densities of 20, 30 and 40 kg/m^3, respectively). For the static loading, pressure was applied at a rate of 1 kPa/s in order to comply with the condition of fully static loading (Moghaddas Tafreshi and Dawson, 2010). For cyclic tests, the loading frequency was 0.1 Hz which is the same frequency of load application as in the full-scale cyclic tests.

6.1.1 Static test results

Fig. 4 displays the measured stress-strain response of the EPS under static loading. The overall shape of the stress-strain curves is similar to those determined in previous studies, consisting of 4 parts including: an initial linear response, yielding, linear + work hardening, and nonlinear + work hardening (Stark et al., 2004). The elastic limit of EPS geofoam is defined as the stress at 1% strain and compressive strength is defined as the compressive stress at 5 or 10 percent strain; the latter is more common (Horvath, 1994). Using this definition, the elastic limit of EPS 20, EPS 30 and EPS 40 are about 8, 22 and 29 kPa and their compressive strengths are about 84, 156 and 244 kPa correspondingly. The subsequent part of the curves (up to about 6~7% strain) is elasto-plastic, comprising a limited amount of plastic strain and therefore, is excluded from the definition of elastic limit. From the elastic part, elastic modulus of the material can be obtained as 0.81, 2.16 and 2.86 MPa for EPS 20, 30 and 40 respectively. All specimens were strained up to 90%. At this ultimate point, EPS 20 could tolerate 350 kPa of pressure, EPS 30 showed a resistance of about 513 kPa and for EPS 40, this ultimate resisting pressure was around 857 kPa.

It is interesting to compare this result with those of other researchers. For example, Horvath (1994) presented a diagram for EPS 21 under short term unconfined axial compression loading. The tests were strain controlled at a rate of 1-20% per minute with 10% per minute as the most common rate. The overall shape of the resulting diagram is very similar to the diagram for EPS 20 derived from current study, however the values show a noticeable difference. For instance, the pressure at 80% vertical strain is 340 kPa in the current tests, while it reaches to about 500 kPa in the mentioned research. A value of approximately 500 kPa is also reported by Bartlett et al. (2015).

Various studies have identified different functions to evaluate elastic modulus and compressive strength of EPS based on their densities. For example, Duskov (1997) proposed a polynomial function of second order to relate initial Young's modulus of EPS with its density. Stark et al. (2004) concluded that a linear regression would be adequate. They have also suggested a linear function for predicting the compressive strength of EPS from its density. Drawing on the data of **Fig. 4**, Equations **(1** and **(2** have been identified respectively to calculate initial Young's modulus and compressive strength of the EPS blocks.

$$E=102.5\,\rho - 1132 \qquad \textbf{(1)}$$

$$\sigma_c = 800\,\rho - 7867 \qquad \textbf{(2)}$$

Where E and σ_c are the initial Young's modulus (kPa) and compressive strength (kPa) of EPS and ρ is density of EPS block (kg/m^3).

The first equation shows a significantly lower initial Young's modulus (E) of EPS geofoam than those presented by Stark et al. (2004), as of $E=450\ \rho - 3000$. Although, it must be noted that the initial Young's modulus obtained here was under slow loading condition, while those reported by Stark et al. (2004) were measured during rapid loading condition. Meanwhile, the coefficients of the second equation (σ_c) are clearly close to the coefficients of equation introduced by Stark et al. (2004). This indicates that the elastic region of the EPS in the current study and under this loading rate (1 kPa/s) is more limited compared to those of similar studies. Hence, the current EPS exhibits a steady transient region from its elastic to its plastic part, while the EPS introduced in other studies shows a sudden transformation from elastic to plastic behavior. In practice, EPS geofoam is seldom designed and evaluated by its elastic modulus, nor is it limited to work in its elastic strain range (1%); but rather, its compressive strength and yield strength (which is also dependent on its compressive strength) are the determining factors for most applications.

6.1.2 Cyclic tests results

To evaluate and quantify the cyclic response of EPS blocks, the three densities of EPS were tested under two or three specific cyclic pressures with a repetition of 100 cycles. The intensities of the cyclic pressure were selected based on the recorded range of pressure values transferred to the top of EPS layer (see section 6.2.3). These values had been logged by the pressure sensor during the mainstream experiments. The response of each density under the selected cyclic pressures would this be truly representative of its behavior in the full-scale test; and the conclusions based on these small scale tests can provide a logical base for interpretation of the overall behavior of the pavement structure in the full scale tests.

Fig. 5 (a) shows hysteresis curves of EPS 20 under cyclic pressure of amplitudes 50, 100 and 150 kPa. It can be observed that EPS 20 shows a stable cyclic behavior for cyclic pressures up to 100 kPa. When the cyclic pressure is 50 kPa, EPS 20 does not strain larger than about 2.3% after 100 cycles; when the cyclic pressure is 100 kPa, vertical strain reaches to 4.47%. It should be noted that when the applied pressure is 100 kPa, the value of strain tends to grow slightly during whole loading procedure, however for 50 kPa, it can be assumed to become totally stable after the first few cycles of loading. For both 50 and 100 kPa loading, it is clear that the major portion of permanent deformation occurs during the first cycle and strain does not significantly increase after this point. When the applied cyclic pressure reaches 150 kPa, EPS 20 turns out to deform very rapidly, such that the vertical strain increases beyond 20%. When loading continued with additional cycles, total and permanent deformations grew even larger.

Comparing **Fig. 5**a with **Fig. 5**b, while EPS 20 shows a maximum strain of about 4.5% at the end of 100 repetition of 100 kPa pressure, this value for EPS 30 is less than 3%. This is reasonable as EPS 30 is stiffer and has a greater yield stress compared to EPS 20. EPS 30 reaches a maximum strain of about 18% after 100 cycles of 150 kPa, whereas EPS 20 deformed severely after the first cycle at this pressure. EPS 40 was not used commonly in the cyclic tests, hence only two cyclic pressures were picked to assess its response. **Fig. 5**c shows that applying 100 cycles of pressure at 200 kPa will generate only a maximum strain as small as 4.3% in EPS 40 after 100 cycles. For EPS 30, the strain under cycles of this stress is definitely greater than 18% (the value at 150 kPa) according to **Fig. 5**b. It is also clear that the strain under this cyclic pressure is very stable and does not grow significantly after the first few cycles of loading.

According to **Fig. 6Error! Reference source not found.**a, EPS 20 strains in a stabilizing manner for cyclic pressures of 50 and 100 kPa, and deforms very rapidly for a cyclic pressure of 150 kPa. Fig **Error! Reference source not found.**b shows that EPS 30 deforms very rapidly under 150 kPa and does not tend to stabilize even after 100 cycles. This kind of intermediate trend is also expected for EPS 20 between 100 and 150 kPa, which has not been determined exactly here. When the amplitude of cyclic pressure increased to 250 kPa, EPS 30 also exhibited a severely unstable behavior and strained up to 28% after the first cycle of loading. These findings indicate that even though EPS 30 is stronger than EPS 20, it shows a rapidly increasing deformation behavior under cyclic pressures larger than 100 kPa. Further tests could be planned with pressures between 100 and 150 kPa to find a threshold for EPS 30, but it was not necessary as the main objective of these small-scale tests was just to obtain an overview about the consequences of using EPS of different densities.

Another important parameter to consider would be the resilient modulus (M_r) of EPS geofoam alone. **Fig. 7** displays the resilient modulus of EPS 20, EPS 30 and EPS 40 each subjected to two different intensities of applied pressure for each EPS density. According to this plot, the resilient modulus of EPS geofoam varies with the amplitude of applied pressure. Considering the stabilized part of the plots (say after the 10th cycle), for EPS 20, M_r rises from 3.2 to about 4.1 MPa with increasing the applied pressure from 50 to 100 kPa. Increasing the applied pressure to 150 kPa causes a reduction in the resilient modulus to less than 3 MPa during the initial applied loading cycles, prior to failure (not shown on the figure). This behavior is in agreement with the trend of behavior observed in **Fig. 5** and **Fig. 6** it can be deduced that as long as the applied pressure is below the stable limit of EPS geofoam, the resilient modulus increases slightly with increase in the applied pressure. With an increase in the applied pressure beyond this limit, an initial increase in modulus appears, followed by the typical steady trend as observed when subjected to other pressures. In addition, the resilient modulus calculated from cyclic tests is generally greater the that obtained from static tests and this value (obtained from cyclic tests) can be considered for design purposes. The inequality of resilient modulus and initial tangent young's modulus resulted observed in these cyclic tests is in agreement with that reported by Stark et al. (2004). The same observations were also made for the other two EPS densities – the stable state resilient moduli for the studied deviator stress values for EPS 30 and EPS 40 were 5.5 and 6.5 MPa, and their lower bound moduli were about 2.64 and 5.5 MPa, respectively.

To summarize, tests on small samples of EPS reveal that when EPS is subjected to cyclic stresses below a certain limit, the amount of permanent deformation is very small, and a major portion of this strain or deformation is resilient. When the cyclic pressure values exceed a certain value (at around the elastic limit), EPS deforms very rapidly and substantially. This threshold pressure is unique for each EPS density after which the resilient modulus also starts to decrease. These findings are also in accordance with the ones presented by Trandafir and Erickson (2012). According to these outcomes and earlier suggestions in the literature, higher densities of EPS were placed directly under the soil layer and above lower density fill of EPS, in order to provide protection and act as a load spreader to reduce pressure and strains in the main part of the embankment (lower-density EPS).

6.2 Behavior of EPS-soil backfill

An initial set of tests were performed in the test box to identify the effect of upper soil layer density, intensity of applied pressure and distribution of stress with depth inside the EPS geofoam body. The tests also allowed the evaluation of the effects of soil thickness, upper EPS thickness and EPS geofoam density.

6.2.1 The influence of backfill soil compaction

First, it is necessary to figure out how the compaction (density) of sand affects its cyclic performance. To this end and for the sake of comparability with installations containing EPS, it was preferred to conduct large-scale plate load tests (Test Series 1 in **Table 4**). For this purpose, soil was placed and compacted in 12 lifts of 100 mm height to reach a total elevation of 1200 mm.

As will be shown in the succeeding sections, the maximum compaction of a 300 to 400 mm soil cover placed over EPS blocks will not produce a dry density higher than 18.7 kN/m^3 (corresponding to 92% of maximum dry density) for 600 to 700 mm thickness, this value can reach up to 19.6 kN/m^3 (corresponding to 96% of maximum dry density). To achieve a similar dry density for the soil alone, several in situ density tests were performed with various amount of compaction energy to determine appropriate compaction method of the sand alone. It was found out that only approximately half as many passes of the compactor were needed for the soil-only lifts to achieve an equal dry density as when the soil was placed over geofoam blocks.

Fig. 8 compares hysteresis curves and settlement of loading surface for the two dry densities described in the previous paragraph. After applying 100 cycles of 275 kPa cyclic pressure, the surface settlement for 18.7 kN/m^3 and 19.6 kN/m^3 cases are about 2 mm and 1.7 mm, respectively. Subsequent application of 400 cycles with 550 kPa amplitude results in a maximum settlement of 6.6 mm and 3.1 mm for these densities, respectively. Although, the reduction of settlement by increasing dry density for low amplitude cyclic pressure is only 15%, this decrease is about 53% for high amplitude load. Consequently, application of a higher compaction energy to attain the maximum dry density can be assumed trivial in many, but not all, circumstances. Depending on the loading that the pavement will carry, special attention to compaction may have to be paid, in order to assure adequate performance.

To investigate this phenomenon in detail, it is also useful to determine the stress values in the soil as shown in **Fig. 8**c. For the sake of comparability with the future tests, a pressure cell was placed at depth of 400 mm in the backfill soil. When the cyclic applied pressure is 275 kPa, the measured pressure is almost identical for both dry densities, ranging between 40 and 50 kPa. By increasing the applied pressure to 550 kPa, a substantial difference shows up in the pressure levels transferred to the depth of 400 mm: the peak value of transferred pressure for lower density and higher density cases were 140 and 80 kPa, respectively. These differences in stress distribution as a function of density and load level are best understood in terms of modulus dependency on stress level. When there is insufficient compaction and sufficient stress so that plastic deformation occurs, then modulus is low, stress is less efficiently distributed and higher peak stress levels are felt vertically beneath the load.

Accordingly, for the 550 kPa stage, the stabilized resilient modulus calculated from tests (as Christopher et al., 2006) were approximately 270 and 230 MPa for higher and lower compaction cases, respectively, and were slightly lower for the 275 kPa applied pressure. These stress-dependent values are comparable to those of typical quarry material and, lower than those of recycled concrete aggregate (e.g. Arulrajah et al., 2013).

6.2.2 The influence of applied pressure amplitude

Test Series 2 and 3 aim to identify the effect of loading amplitude on settlements of the surface of pavements including EPS and to determine the pressure transferred to the upper EPS layer. A typical soil thickness of 400 mm was used in this Test Series (Swedish standard, 1987; Norwegian standard, 1992). The thicknesses of upper and bottom EPS layers were selected as 200 mm and 600 mm with densities of 30 and 20 kg/m^3, respectively. Each layer of soil above the EPS was compacted to its maximum achievable compaction (18.7~19.6 kN/m^3). The test was performed with load amplitudes of 400 and 800 kPa, which are the pressure amplitudes that might be applied to the pavement surface (of unpaved roads). The other pressure amplitudes were 275 and 550 kPa representing reduced pressure values anticipated on the soil beneath the asphalt cover layer in a paved road.

Fig. 9a and b illustrate the hysteresis curves for the specified tests. It indicates that while the reduced load (275 and 550 kPa) can hardly produce a settlement larger than 25 mm in the loading surface after a total of 500 loading cycles, the original pressure (400 and 800 kPa) can trigger up to 70 mm settlement in the loading surface after applying only 200 load cycles. The test was terminated at this surface settlement so as to prevent excessive settlement and possible damage to the pressure cell.

Fig. 9c depicts the value of transferred pressure on the first layer of EPS. When the applied pressure is 550 kPa, the transferred pressure is about 120 kPa which is perhaps below the limit of unstable permanent deformation of the EPS 30 as shown in **Fig. 5**b. For 800 kPa, the conveyed pressure is larger than 200 kPa, which is well beyond the 150 kPa limit of instability for EPS 30. As the cyclic tests on EPS samples showed, when the applied pressure over geofoam becomes excessive, the EPS very rapidly exhibits large strains with a slight increase in the pressure. Furthermore, as shown earlier in this section, the soil may not then be capable of spreading the applied load so effectively, transferring it to the EPS.

Variation of resilient modulus for soil and EPS geofoam was investigated separately in the previous sections. To observe the resilient modulus under the combined effect of soil and EPS geofoam, Fig. 9d should be viewed. During application of 400 kPa cyclic pressure (400kPa for 100 cycles then 800 kPa loading scenario) M_r stabilized at 13 MPa but then decreased to ~10 MPa under the subsequent cyclic pressure of 800 kPa until failure happened. This particular level of resilient modulus corresponds to a very short service life for the pavement, unless proper base and subbase courses are considered above them. The other loading scenario (275kPa for 100 cycles then 550 kPa) exhibits a better behavior, with a resilient modulus 27 and 17 MPa during the lower and higher applied pressures, respectively. While separate examination of the EPS 30 and the soil yielded resilient moduli of the order of 5 MPa and 200 MPa for them respectively, the combined assembly of these two materials has resulted in resilient moduli of 17 and 27 MPa at the two loading pressures. The reason for such low resilient modulus of the composite pavement system is the inability of EPS geofoam to provide sufficient support for the 400 mm soil above it, preventing mobilization of adequate confining pressure that would otherwise enable higher resilient moduli in the soil (Duskov, 1997).

Thus, using EPS geofoam for roads requires the designer to limit the pressure transferred to the EPS layer so as to keep the deformations of the pavement surface in a tolerable range. For unpaved systems, this implies a substantial increase in thickness of soil layer above the EPS blocks and paying attention to the density of the compacted soil. Of course, this may introduce undesirable increases in dead load and/or in construction time. For paved roads on the other hand, an asphalt layer with a typical thickness of 50 mm would deliver a definite improvement (reduction) in deformation of the system and in the pressure imposed on the EPS (46% in this study based on **Fig. 9c**). In most cases, a thicker asphalt layer might be used with even greater reduction in the pressure value.

6.2.3 Variation of pressure with depth in EPS layers

Four confirmatory tests were carried out to guarantee that the pressure transmitted to the bottom of the box is negligible (Test Series 3 from **Table 4**). Similar to Section 6.2.2., the tests were performed on 400 mm of soil cover placed over four layers of EPS geofoam blocks, each with a thickness of 200 mm. The density of the uppermost EPS layer was 30 kg/m^3 (EPS 30) and the remaining layers were formed of EPS 20 (density of 20 kg/m^3). The pressure sensor was placed on the top of the top EPS layer and between the EPS layers. In this Test Series, 100 cycles of 275 kPa were followed by 400 cycles of 550 kPa load applied to loading surface. The condition and parameters' values for all of the above tests (except the location of pressure cell) were the same. As the surface settlements were closely replicated for the all the tests (regardless of depth of the pressure cell) only the surface settlement of the test with the pressure cell at a depth of 40 mm is shown in **Fig. 9**.

Fig. 10 shows the variation of vertical pressure with depth below the loading surface. At the boundary of the soil and the first layer of the EPS (at a depth of 400 mm), the maximum pressure is about 122 kPa, about 22% of the applied surface pressure of 550 kPa. Under the first layer of EPS geofoam (at a depth of 600 mm), the pressure drops to about 15% of the surface loading pressure, a further 37% reduction from its value at the top of the EPS 30 (400mm above). By a depth of 800 mm, the pressure is only 7% of the surface pressure (a 56% decrease over the last 200mm thickness of EPS) and by a depth of 1000 mm, the stress is only 4% of the surface pressure having reduced to 18 kPa (a 47% reduction across the EPS). The role of the soil in providing the initial stress distribution is, thus, apparent. At the bottom of the box, the pressure is about 15 kPa, compared to 18kPa at the top of the lowest EPS layer – i.e. the bottom EPS layer doesn't achieve much load spreading and, at such a low stress level, won't compress much (c 1.38 mm using the EPS results presented earlier). This confirms the adequacy of the box's vertical dimensions.

Yet, it appears that EPS geofoam transfers pressure vertically rather than horizontally. This can be explained in terms of the low Poisson's ratio and non-particulate structure of this material. Granular material such as soil can effectively redistribute pressure in the horizontal direction due to interlocking of the particles, while geofoam bubbles are compressive and tending not to expand laterally and, thus, cannot appropriately transfer the pressure in the horizontal direction. Because of this characteristic, EPS geofoam undergoes very little or even zero lateral expansion (or even contraction due to bubble collapse) when subjected to deviator compressive pressure and induces significantly lower lateral pressures than normal earth pressures (Wong & Leo, 2006).

6.2.4 Combined effect of soil and upper EPS layers' thickness

Test Series 4 (see **Table *4***) was arranged so as to study the influence of variation in the soil and upper EPS layer thicknesses on the settlement of the loading surface and the pressure transferred through the soil and the top EPS layer. A layer of low density EPS (here 400 mm of EPS 20) was placed at the bottom of test pit and the remaining part of the pavement was filled with a high density EPS (here EPS 30) and a layer of soil. The thickness of the soil layer (h_s) and thickness of the upper EPS layer (h_{gt}) were varied within a total constant, thickness, of 800 mm.

Fig. 11a displays total (peak) and residual deformations of the loading surface for different values of h_s and h_{gt} under 100 cycles of 275 kPa followed by 400 repetitions of 550kPa. The figure indicates that when h_s is lower than 300 mm, the pavement will undergo severe settlement after just 150 cycles. At this point, total settlement rises to 68.5 mm and the amount of permanent (residual) settlement is 52.5 mm (**Fig. 11**b). For larger values of h_s, this rapid and unstable growth in total and permanent deformation are not observed and the pavement behaves predictably for 500 load cycles. However, the degree of stability and rate of increase in total and permanent settlements is not similar among them. Although the increase in rate of deformation is negligible for h_s=700 mm, the remaining cases show an increase in the deformation during cyclic load application. If h_s is smaller than 400 mm, the pavement deformation will certainly pass 25 mm, a typical maximum allowable rutting at the surface of a low volume road (Qiu et al., 2000). On the other hand and as shown in **Fig. 11**b, a maximum rut depth of 50 mm for low volume roads and 30 mm for major roads is suggested by AASHTO T 221-90, criteria that would be met for low volume roads so long as $h_s \geq 300$mm whereas $h_s \geq 400$mm might be needed for major roads at larger numbers of cycles.

An extended clarification can be obtained by reviewing the pressure variation over the upper layer EPS blocks. According to **Fig. 11**c, for h_s=600 mm and h_s=700 mm, the peak pressures applied to the upper EPS layer are about 64 kPa and 37 kPa, respectively. These values are well below 100 kPa which was found as a potential upper limit for stabilized behavior of EPS 30 (**Fig. 5**b or **Fig. 6Error! Reference source not found.**b). When the pressure transferred to the EPS is around or higher than 100 kPa (in the case of h_s<=400 mm), EPS can be expected to deform at a very rapid rate, based on the earlier tests performed on the EPS specimens. Thus, from a pressure point of view, Fig 11c confirms that a soil thickness of >400 mm can be desirable in order to limit large EPS deformation under a surface stress of 550 kPa.

The effect of the soil and upper EPS layer on the resilient modulus is presented in **Fig. 11**d. As expected according to this plot, with increasing soil thickness, the resilient modulus increases. When the pavement is subjected to the first 100 cycles of 275 kPa pressure, the resilient moduli for h_s=700, 600, 400, 300 and 200 mm are 115, 80, 40, 27 and 13 MPa, respectively. During the second loading stage (550 kPa applied pressure), the corresponding resilient moduli decrease to 50, 30, 21, 17 and 7 MPa, respectively. While a designer might find $h_s \geq$ 300 mm and its corresponding resilient modulus appropriate for a subgrade subjected to the lower pressure (20.7 MPa as of Christopher et al., 2006), a soil thickness of at least 600 mm might be required to satisfy typical requirements for resilient modulus of subgrade. According to this approach, the EPS geofoam must be used when the natural ground is extremely weak, otherwise in cases with sufficient strength of subgrade, EPS geofoam must be evaluated against other possible alternatives, such as bridges or soil improvement methods (Izevbekhai & Pederson, 2011).

Although AASHTO 1993 recommended a lower limit for the resilient modulus of the subgrade, no such criterion is required by the mechanistic-empirical (MEPDG 2008) approach – it simply considers various cracks types and ruts as performance indicators. Nevertheless, Boone (2013) examined the effect of several factors including resilient modulus on the distress response of the pavement in the Ontario area and warned that base resilient modulus and subgrade resilient modulus are among several distress indicator factors that would impact bottom-up fatigue cracking and top-down fatigue cracking, respectively. So in terms of resilient modulus, the compacted soil and EPS 30 layers of 400 and 200 mm thicknesses, respectively, placed over EPS 20, require a thicker asphalt layer (thicker than 50 mm of 2.5 GPa asphalt layer) in order to prevent premature failure. Otherwise, only lighter trucks should be allowed to pass, or the service life will drop significantly.

To summarize the influence of soil thickness and the relating mechanisms on the pavement settlement, ultimate values of peak and residual settlements of the loading surface are compared for different values of soil thickness in **Fig. 12**. When the lower pressure of 275 kPa is applied to the loading surface, the variation of maximum settlement does not change significantly, and it is negligible when h_s is below 400 mm. It is also clear that the peak and residual deformations are very close at this point, meaning that the majority of deformation is recoverable. For a cyclic load of 550 kPa, a noticeable variation in the peak and residual deformations can be perceived with respect to h_s and the difference between peak and residual deformations is clear.

Based on the peak settlement profile of loading surface shown in **Fig. 13**, the maximum peak deformation of the loading surface was 75 mm for the soil layer thickness of 200 mm and the deformation for the other thicknesses of soil are, evidently, much lower. It is commonly expected that the area of soil deforming would increase with increase in depth of settlement due to the extension of the failure surface in the soil and/or the beam-type deflection of an upper foundation layer. However, in these tests, the deformation 'bowl' hardly extends beyond the edge of the loading plate for any soil thickness (**Fig. 13**). This indicates a punching mechanism under the loading plate for the pavements constructed on soil-over-EPS layers. Previous research (Ossa & Romo, 2009; Lingwall, 2011) have demonstrated that EPS geofoam shows a very small negative Poisson's ratio in its elastic region and a negative dilation angle in its plastic region. Ossa & Romo (2009) described that when the foam is compressed in three dimensions, the cellular volumes of air bubbles destruct and the internal structure of the foam buckles, resulting in lateral contraction of the material. This phenomenon leads to decrease in the strength of EPS with increase in the confining pressure and causes the material to deform in a punching manner. Therefore, it might be expected that EPS geofoam will not obey the rules of common analytical methods (at least in part), as will be discussed further in Section 7.

The larger surface settlements occurring for lower thicknesses of soil cover over the EPS layers are not exclusively a consequence of the thinner soil layers, but also due to the lower stiffnesses of those soil layers. As reported earlier, when the thickness is <400mm, the dry density of the soil reached a maximum value of 18.7 kN/m^3, whereas for 600~700 mm soil, the soil can be compacted to a dry density of 19.6 kN/m^3. This is related to the low mass and stiffness of EPS geofoam which does not provide an adequate base on which the soil mass can be compacted. Lower stiffness is expected to be associated with this lower compaction thus achieving less load spreading and, hence, greater stress and settlements than would otherwise have been the case will be experienced immediately beneath the load.

6.2.5 Combined effect of upper and bottom EPS layers' thickness

In this section, the results of Test Series 5 are described. As discussed previously, a slight reduction in EPS usage can make a significant reduction in the cost of a highway project. Also, the cost effectiveness of an EPS backfill would be significantly affected by the thickness of the upper, higher density, EPS layer. In addition, if the thickness of such an upper EPS layer is too small, the safety of the pavement structure might be endangered due to out-of-specification deformations in the pavement. Hence, the optimum thickness of a high-density, upper, EPS layer has to be specified correctly.

Fig. 14 illustrates the results of experiments on sections with different values of h_{gt} and h_{gb}. In part (a) of this diagram, it is clear that when h_{gt} is 100 mm, settlement of the loading surface increases rapidly. It was observed that the upper EPS layer broke into two parts after the test, which can be supposed as the main reason for this dramatic increase in surface settlement in this test. However, it seems that rupture of the EPS block has not happened instantly after only a few cycles of loading, rather it happened gradually during loading. Observations from other tests suggest that when EPS blocks bend too much, invisible or very small cracks are generated in the tension region of the block (in this case, the bottom of the block), then the cracks develop under subsequent loading cycles and, eventually, the block ruptures fully or partially. For thicker blocks however, the height of the section and its moment of inertia increases. This action helps to reduce tensile stress at the bottom of the upper EPS block and, hence, will extend its bending resistance to more repetitions of loading.

Fig. 14b displays peak settlements extracted after 500 repetitions of low and high intensity pressures (it is extracted at load cycle of 150 for the case of h_{gt}=100 mm and h_{gb}=700 mm due to that test's early failure). When h_{gt} is less than 200 mm, peak surface settlement has increased to 57 mm. When h_{gt} is equal to or greater than 200 mm (200 mm to 600 mm), peak value of surface settlement remains between 17.4 mm to 23.7 mm, with very small variation, and a large drop from the settlement corresponding to h_{gt}=100 mm. Thus h_{gt}=200 mm is approximately a minimum value for the upper EPS layer under this loading. Thickness values of the upper EPS layer larger than 200mm would increase construction costs without delivering noticeable benefit in the reduction of settlements.

6.2.6 Effect of EPS density (EPS stiffness)

The influence of EPS density on the permanent deformation was explored in Test Series 6. With this aim, the density of EPS in both the upper and lower layers was changed and the cyclic plate load test was repeated for each section. Values of h_s, h_{gt} and h_{gb} were kept equal to 400, 200 and 600 mm, respectively. Based on **Fig. 15**, the amplitude of settlement in the loading surface are stabilized below 6 mm after application of several cycles of low amplitude pressure for all cases.

For the higher amplitude of applied pressure, the settlement of the loading surface rises but stabilizes quickly when the density of upper and bottom EPS layers are 40 kg/m^3 and 40 kg/m^3 or 30 kg/m^3 and 30 kg/m^3, respectively. For 40-40, maximum settlement was limited to 9.6 mm and for 30-30, this value was about 11.4 mm at the end of tests. The settlements for these two cases are significantly lower than those of EPS 30 over EPS 20. Therefore, the lower stiffness of EPS 20 is implicated as the cause of larger settlements induced in the pavement surface. As discussed previously, the initial resilient modulus of EPS 20 is about 3~4 MPa, which means that most of such EPS enters its plastic region and deforms excessively compared to EPS 30 and EPS 40 at similar depths. However, such deformation is localized and limited to a small horizontal surface of EPS and could be reduced if proper load distribution mechanisms are used. EPS 20 over EPS 20 shows extreme deformation after a limited number of pressure application and is not suitable at all.

7 Discussion of results

The following concluding remarks result from the specific EPS geofoam and the properties of soil used for the tests. If the condition of the real project varies from these, the performance of pavements might vary depending on the materials and preparation procedure. In general, for the tested loading amplitudes of 275 and 550 kPa, the soil layer placed over EPS blocks should not be selected thinner than 400 mm in order to prevent excessive permanent deformation, or less than 400 and 600 mm in order to maintain adequate resilient modulus support for the higher layers under 275 and 550 kPa pressures, respectively. Nevertheless, soil thicknesses of 400 and 600 mm can be selected as appropriate lower and upper bounds, as the mechanistic-empirical approach has not limited the resilient modulus.

For the experiments reported above, when the thickness of soil layer is less than 400 mm, the transferred pressure on top of EPS layers increased beyond the safe stress limit of EPS 30, which resulted in progressive increase in the strain of EPS layer. Therefore, the shear strain in the soil above the blocks increased until the soil failed in punching.

The thickness of the upper EPS layer is also influential and should not be lower 200 mm when the soil thickness is 400 mm, as the EPS block will rupture and cannot bear further pressure. The tensile strains start to grow in the soil layer above the cracked zone of EPS blocks, which results in shear or tensile failure of the whole soil layer, leading the pavement to undergo severe deformations at its surface. Therefore, the thickness of the upper EPS layer with a density of 30 kg/m^3 (the denser EPS) could be limited to as little as 200 mm, with a minimum covering soil thickness of 400 mm. Large thickness is not required for the upper EPS layer, as the further improvement in performance of pavement is small compared to the increase in cost of the project. Increasing the density of the bottom EPS layer significantly reduces rut depths (although, for the cases investigated, the rut would already be acceptable, before this increase), but is not recommended due to the extreme increase in project cost.

To summarize, a properly compacted layer of soil of thickness 400 mm placed above an upper EPS layer with a density of 30 kg/m^3 and a minimum thickness of 200 mm, in its turn placed on a bottom layer of EPS with a density 20 kg/m^3, would satisfy the range of settlements or rut depths for “low volume” and “major” roads (30 mm and 50 mm, respectively), as dictated by AASHTO T 221-90.

Given that the experiments could only investigate a few of the many possible scenarios of use, the distribution of pressure in EPS layers and the likely settlement of the pavement surface, was investigated using simple analytical methods based on elasticity theory. Linear and nonlinear methods based on Burmister’s layered theory, as implemented in the KENPAVE software, are available for such a purpose (Huang, 1993). While a major part of the current test results (specifically those under cyclic pressure of 550 kPa) are plastic in nature, the results obtained for lower cyclic pressure (275 kPa) can be assumed as linear or nonlinear elastic, especially in the first cycle of loading – and it is elastic behavior that is required in a satisfactory installation. Therefore, an elastic analysis should be able to define the arrangements that deliver the limiting acceptable stresses for practical application although it would be incapable of predicting stresses and strains beyond this limit.

In both linear and non-linear methods, it is required to estimate the resilient modulus (or initial resilient modulus in the case of nonlinear method) of soil using the results of test performed on the soil alone. Simulation of the first cycle of loading of the test described in Section 6.2.1 using the linear method of KENPAVE gave a modulus of about 55 MPa for the soil alone. Moduli of upper and bottom EPS materials were equal to 2.16 and 0.81 MPa (see Section 6.1.1). These values were doubled based on the results of the study by Negussey (2007), so as to obtain reasonable results. Therefore, these values can represent an equivalent elastic medium and provide an approximate implementation of the real system.

Using the nonlinear method in KENPAVE, a better estimation might be achievable. In this method, soil resilient modulus is related to the first stress invariant using a simple equation as (Huang, 1993):

$$E=K_1\,\theta^{K_2} \quad \textbf{(3)}$$

where θ is the first stress invariant and K_1 and K_2 are calibration factors obtained from experiments.

According to the observation reported by Uzan (1985), modulus for a soil should decrease with increase in the first stress invariant, θ, therefore K_2 will be negative. This approach was also adopted for EPS geofoam at subsequent layer and by the use of proper calibration factors shown in **Table 5**, the desired results were obtained.

The results for both the linear and nonlinear analyses, compared with the values measured in the experiments, are shown in **Table 6**. As shown in this table, the linear analysis gave a surface deflection of 2.5 mm and the pressures at depths of 400 mm and 600 mm were equal to 14.9 kPa and 7.5 kPa, respectively. The variation from the experimentally measured value is -38% in the case of surface settlement and equal to -55% to -66% for the transferred pressures. Using the nonlinear method, the surface settlement was calculated as 3.8 mm (-5 %

deviation) and the pressures at depths of 400 mm and 600 mm were 38 kPa (+15% deviation) and 11.4 kPa (-22% deviation).

Comparison of different methods for calculation of transferred pressure at different layers of EPS is also depicted in Fig. 17. Although Boussinesq provides reasonable estimates of stress for depths greater than 400 mm, its result is far from the measured value at a depth of 400 mm (a +49% deviation). KENPAVE linear significantly underestimated results whereas the nonlinear method already gives a much closer match from a general point of view. Overall, it is clear that a simple linear analysis is inadequate for such a pavement system and further studies including model tests or high accuracy nonlinear analysis might be needed to determine deflections and pressure with higher reliability. For the full range of depths, the KENPAVE nonlinear method gives the most accurate result of those evaluated.

Fig. 17a shows the effect of variation in initial soil resilient modulus (using the KENPAVE nonlinear method) on the pressure transferred to the surface of upper EPS layer, considering both EPS 30 and EPS 20 as the top layer. In this figure, the horizontal dashed lines indicate approximate threshold stress for stable response of EPS 30 and EPS 20 obtained from cubic sample tests. These values from tests were about 100 kPa and 50 kPa which were halved to provide a safety factor against unstable response of EPS geofoam. The measured point from the tests (Section 6.2.3) is close to the obtained curves, so the somewhat crude KENLAYER analysis may be useful. The figure shows that, with the EPS30, a soil with a modulus of less than 25 MPa (the vertical dashed arrow on **Fig. 17**a) can’t be used as the stress at the top of the EPS would be too large for that EPS, i.e. > 50kPa. With EPS20 as the upper layer (the total height composed of EPS20), none of the soil moduli deliver a safe stress when the soil thickness is 400 mm. This EPS density must be avoided from application as upper EPS layer. However, it must be remembered that the tolerable stress margins were halved. If the real stress margin (50 kPa) for EPS 20 is considered, soil with K_1>30 MPa could be considered as acceptable, which is in agreement with the test results (see 6.2.6).

This approach could be easily repeated for other moduli and thicknesses of soil and EPS and for other loadings to determine the amount and quality of soil cover that is needed. To this aim, a sensitivity analysis on the effect of applied pressure, soil and upper EPS layers’ thicknesses and upper and bottom EPS thicknesses analysis was performed. **Fig. 17**b depicts the effect of loading intensity on the transferred pressure to the upper EPS layer with considering different K_1 values. The thickness of soil, upper EPS layer and bottom EPS layers were 400 mm, 200 mm and 600 mm, respectively and either EPS20 or EPS30 were used in the upper EPS layer. The figure indicates that for the applied pressure up to 275 kPa, all of the investigated cases are acceptable when

EPS 30 is placed as the upper EPS layer. As K_1 values are increased, the pressure transferred onto the EPS layers' decreases. For instance, when EPS 30 forms the upper layer, the maximum allowable applied pressure for K_1=20, 40 and 60 MPa would be about 250 kPa, 310 kPa and 360 kPa, respectively. As before, using EPS 20 as the top layer failed to deliver acceptable behavior over the full range of applied pressure amplitudes.

The combined effect of soil and upper EPS layer is shown in **Fig. 17**c. The trend in the variation of the intensity of transferred pressure onto the upper EPS layer varies with the variation in soil stiffness (K_1) and soil thickness. As a general understanding, a low value of soil stiffness (e.g. K_1=20 MPa) must be avoided. For higher values of K_1 though, a slight increase in the applied pressure can be observed at a depth of 400mm (i.e. poorer load spreading) with increase in soil thickness relative to upper EPS layer. **Fig. 17**d displays the effect of upper and bottom EPS layers thicknesses while the thickness of soil was kept constant and equal to 400 mm. It can be seen that, when the thickness of upper EPS layer increase relative to the thickness of bottom EPS layer, the pressure slightly increases and remains constant beyond an EPS thickness of around 400mm.

The above discussion implies that for the specific kind of soil and EPS geofoam (or any similar material) used in this study, a rutting and transferred stress evaluation can be made of the effect of several factors, including soil and upper EPS layer thicknesses, density of EPS forming the top and bottom layers and applied surface pressure. A significant variation from the mentioned material characteristics might alter the predictions in a unfavorable way and hence, the application of the results must be extended with great care. Further investigation is certainly needed to discover some of the remaining issues including:

- a more rigorous characterization of the EPS's installed, as opposed to in-isolation, properties;
- the effect of the different potential EPS materials on the compaction of the covering soil layer,
- the stress distribution and the mechanism of possible failure at different amplitudes of cyclic pressure.

Nevertheless, the results of this study bring deeper insight regarding the performance of pavements including EPS geofoam and improve our appreciation of the EPS-soil-load interaction effects. They show that the soil and upper EPS layer need to be considered together to ensure that the stress passed down from traffic through the soil to the EPS can be reduced to tolerable levels (i.e. sufficiently small to avoid EPS failure). Fig 16c suggests that, other than for light trucks, bound pavement layers will be required, perhaps with a very deliberate load spreading strategy if heavy truck loading is to be used and the weight benefit of EPS is to be obtained over a significant height of the embankment. Otherwise there will be need for substantial thicknesses of covering soil (which opposes the purpose of using EPS) or high stress capacity EPS geofoam (with much greater load competency than EPS30).

8 Summary and conclusion

Several methods are available to reduce the dead load of road embankments and their consequent settlements over weak grounds. Among them, EPS has the additional advantage of its extremely light weight, which leads to much faster construction. However, further study and investigation regarding some of the details about EPS geofoam backfills is required in order to cover current knowledge gaps. Such studies will also aid the development of appropriate standards for the design and building of EPS geofoam embankments.

In the research reported here, several factors were studied in order to gain a deeper understanding about their response to loading. Cubic samples of EPS geofoam were first tested under uniaxial static and cyclic loading conditions in order to evaluate the behavior of that component alone. For soil, cyclic plate load tests were performed with surface settlements and vertical pressure inside a model embankment being recorded. The following results are highlighted:

(1) The engineering properties of EPS of relevance can be expected to vary with supplier, EPS density and application. Therefore, the properties of the actual material to be used should be determined, as far as possible in the manner it is to be applied. For example, the Elastic moduli of EPS from static tests in this study are a lower compared to those of some the previous studies, while their compressive strength shows a good match with prior research.

(2) The static Elastic moduli of EPS and its cyclic Resilient moduli do not agree. For EPS 20, 30 and 40 studied, the static Elastic moduli (at 1% strain) of the three EPS qualities were 0.81, 2.16 and 2.86 MPa, while their stabilized cyclic Resilient moduli were 4.1, 5.5 and 6.5 MPa (at 100, 100 and 200 kPa load levels), respectively. Therefore, under the stabilized condition of cyclic loading application, the resilient modulus of EPS has increase 89%, 154%, 127% for EPS 20, 30 and 40, respectively. As a general observation, it can be said that the cyclic resilient moduli of EPS geofoam can be doubled compared to their static elastic moduli.

(3) The amount of EPS's cyclic Resilient moduli depends on the amplitude of the applied pressure. With increase in the applied pressure, resilient moduli slightly increase until the onset of non-stabilizing behavior. At this point, the amount of resilient modulus starts to drop. For EPS 20 in this study, with increase in the applied pressure from 50 to 100 kPa, its resilient modulus increased from 3.2 to 4.2 MPa and then decreased to less than 3 MPa with further increase in the amount of applied pressure. The

Resilient modulus of EPS 30 dropped from 5.5 to 2.64 MPa when increasing the applied pressure from 100 to 150 MPa.

(4) Compactibility of soil layers overlying EPS blocks depends on the proximity of the two materials. For a thickness of 300~400 mm of soil layer placed over EPS geofoam blocks, the maximum dry density of soil might be around 5% less than it would be in a layer around 600~700 mm thick. Along with this, the resilient modulus of the thinner soil layer above the EPS blocks can be 15% lower compared to its value in thicker soil.

(5) If an unpaved road consisting of EPS layers is subjected to the cyclic loading of heavy trucks (800 kPa), deep ruts will certainly occur on the pavement surface and the operational life of the pavement will considerably decrease due to punching failure in the soil as a consequence of crushing of the EPS. However, the additional load transfers likely to be achieved by providing a bound, sealed surface, can be expected to reduce the stress in the soil and on top of the EPS to a level where the system can tolerate a large number of load repetitions.

(6) The Resilient modulus of the composite system comprising soil and EPS layers depends on the thickness of the soil layer and the loading intensity. While the resilient modulus of the studied soil and the EPS geofoam are of the order of 200 and 5 MPa respectively, for a pavement consisting of 400 mm soil placed on subsequent layers of EPS 30 and EPS 20, the resilient moduli varies between 10 and 27 MPa for an applied pressures of 800 to 275 kPa.

(7) The pressures likely to be applied by a light truck (c275 kPa) induced a peak rut depth of 10 mm on the pavement surface and is insufficient to produce large ruts on the surface of a pavement that includes EPS geofoam. However, pressure from the tires of a heavy truck (c550 kPa) applied on pavement with 600 mm soil thickness are likely to generate up to 27 mm rut after 500 applications, which is due to internal stresses that exceed tolerable limits.

(8) The thickness of the soil layer covering the EPS geofoam bed is a key factor affecting the value of settlements experienced at the loading surface. The compaction (and, hence, the shear strength) of soil placed on the EPS backfill is dependent on the thickness of soil layer placed on the top of EPS geofoam. Therefore, the value of h_s affect the settlements in a duplicated way including the “thickness” itself and the achievable “compaction”. For example, when h_s is equal to 200 mm, the pavement surface deforms excessively under heavy truck load and cannot resist a large number of pressure applications.

(9) In order to find an optimum thickness for soil and upper EPS layer (a cost effective and time saving solution), h_s and h_{gt} were varied in a way that their total value was kept constant. For a medium thickness of soil (h_s =300mm) the surface deformation after 500 cycles of load reduced by 14, 41 and 65% as the soil thickness was increased by 33, 100 and 133%, therefore optimizing soil thickness is critical. The desired value can be selected based on the design priorities and economic factors. For all of the cases, the residual (plastic) surface settlement was about 78% of the total settlement.

(10) As denser, more load resistant, EPS geofoam is costlier then the less dense type, a key design goal is to determine the thickness of upper and bottom EPS layers. With a reasonable soil cover (h_s=400 m), increasing the thickness of a denser and stiffer upper EPS layer from h_{gt}=200 mm to h_{gt}=600 mm only caused a 20% decrease in the total settlement of loading surface. On the other hand, reduction of h_{gt} lower than 200 mm, will induce extreme ruts on the pavement surface due to the rupture of that upper EPS layer.

(11) Density of EPS in the subsequent layers has critical influence on the performance of the EPS embankment. Using EPS 40 for upper and bottom EPS layer can reduce the depth of surface ruts up to 60% after total application of 500 load cycles, with respect to EPS 30 and 20 as top and bottom layers. When the top and bottom layers are EPS 30, the mentioned reduction is 52%. However, application of upper and bottom densities of 40 kg/m^3 over 40 kg/m^3 or 30 kg/m^3 over 30 kg/m^3 and are not practical, and will increase the costs of the project. The case of 20 kg/m^3 EPS placed over 20 kg/m^3 EPS is insufficient for application against 550 kPa and deforms excessively after a limited number of application of cyclic pressure.

(12) An initial stress analysis was performed to investigate the sensitivity of the stress applied to the top of the EPS geofoam. It showed that there will be limiting moduli and thicknesses for the overlying soil. Therefore, it will be important to ensure a well-compacted and carefully selected overlying soil of adequate thickness to ensure that the EPS isn't overloaded and, thereby, prone to punching failure. The exact thicknesses and stiffnesses will depend on materials employed.

This study should enhance appreciation of the behavior of EPS geofoam block in road and highway backfills under the cyclic application of traffic pressure. However, the results are based on large scale plate load tests performed on one type of EPS geofoam (originated from one specific molder), one type of soil, one loading frequency and one loading plate size. Therefore, a generalized conclusion should not be made and it is recommended that the outcomes be used and disseminated with great caution and the limitations for practical application fully considered. A full design method will require more advanced analysis and a wider range of material characters.

Nomenclature

D (mm)	Diameter of Loading Plate
h_s (mm)	Thickness of soil layer
h_{gt} (mm)	Thickness of upper EPS geofoam layer
h_{gb} (mm)	Thickness of bottom EPS geofoam layer
γ_{gb} (kg/m^3)	Density of bottom EPS geofoam layer
γ_{gt} (kg/m^3)	Density of upper EPS geofoam layer
γ_s (kN/m^3)	Density of soil
E (MPa)	Young's modulus
M_r (MPa)	Resilient modulus
K_1	First calibration parameter for nonlinear analysis
K_2	Second calibration parameter for nonlinear analysis

9 References

AbdelSalam, S.S. & Azzam, S.A. (2016). Reduction of lateral pressures on retaining walls using geofoam inclusion. Geosynthetics International, **23,** No. 6, 395-407.

American Association of State Highway and Transportation Officials (AASHTO). (1990). Repetitive static plate load tests of soils and flexible pavement components for use in evaluation and design of airport and highway pavements. AASHTO T 221-90.

American Association of State Highway and Transportation Officials (AASHTO). (1993). AASHTO guide for design of pavement structures.

American Society for Testing and Materials. (2000). Standard Test Method for Compressive Properties of Rigid Cellular Plastics. ASTM D 1621-00.

American Society for Testing and Materials. (2004). Standard Specification for Rigid Cellular Polystyrene Geofoam. ASTM D 6817-04.

American Society for Testing and Materials. (2005). Standard Guide for Use of Expanded Polystyrene (EPS) Geofoam in Geotechnical Projects. ASTM D 7180-05.

American Society for Testing and Materials. (2008). Standard Test Method for Apparent Density of Rigid Cellular Plastics. ASTM D 1622-08.

American Society for Testing and Materials. (2009). Standard Test Method for Repetitive Static Plate Load Tests of Soils and Flexible Pavement Components, for Use in Evaluation and Design of Airport and Highway Pavements. ASTM, D 1195-09.

American Society for Testing and Materials. (2009b). Standard Specification for Graded Aggregate Material for Bases or Subbases for Highways or Airports. ASTM. D 2940-09.

American Society for Testing and Materials. (2011). Standard Practice for Classification of Soils for Engineering Purposes (Unified Soil Classification System). ASTM International, West Conshohocken, PA. D 2487-11.

American Society for Testing and Materials. (2012). Standard Test Methods for Laboratory Compaction Characteristics of Soil Using Modified Effort. ASTM. D 1557-12.

Anil, O., Erdem, R.T. & Kantar, E. (2015). Improving the impact behavior of pipes using geofoam layer for protection. International Journal of Pressure Vessels and Piping, 132-133, 52-64.

Arulrajah, A., Piratheepan, J. & Disfani, M. (2014). Reclaimed asphalt pavement and recycled concrete aggregate blends in pavement subbases: laboratory and field evaluation. Journal of Materials in Civil Engineering, **26**, No. 2.

Arulrajah, A., Piratheepan, J., Disfani, M., & Bo, M. (2013). Resilient moduli response of recycled construction and demolition materials in pavement subbase applications. Journal of Materials in Civil Engineering, **25**, No. 12.

Arulrajah, A., Yaghoubi, E., Wong, Y.C. & Horpibulsuk, S. (2017). Recycled plastic granules and demolition wastes as construction materials: Resilient moduli and strength characteristics. Construction and Building Materials, **147**, 639-647.

Athanasopoulos, G.A., Pelekis, P.C. & Xenaki, V.C. (1999). Dynamic Properties of EPS Geofoam: An Experimental Investigation. Geosynthetics International, **6**, No. 3, 171-194.

Barrett, J.C. & Valsangkar, A.J. (2009). Effectiveness of connectors in geofoam block construction. Geotextiles and Geomembranes, **27**, 211-216.

Bartlett, S.F., Lingwall, B.N. & Vaslestad, J. (2015). Methods of protecting buried pipelines and culverts in transportation infrastructure using EPS geofoam. Geotextiles and Geomembranes, **43**, No. 5, 450-461.

Beju, Y.Z. & Mandal, J.N. (2017). Combined Use of Jute Geotextile-EPS Geofoam to Protect Flexible Buried Pipes: Experimental and Numerical Studies. International Journal of Geosynthetics and Ground Engineering, **3**, No. 32.

Boone, J.N. (2013). Comparison of Ontario Pavement Designs Using the AASHTO 1993 Empirical Method and the Mechanistic-Empirical Pavement Design Guide Method. University of Waterloo.

Brito, L.A.T., Dawson, A.R. & Kolisoja, P.J. (2009). Analytical Evaluation of Unbound Granular Layers in Regard to Permanent Deformation. Bearing Capacity of Roads, Railways and Airfields. 8th International Conference, (pp. 187-196).

Christopher, B.R., Schwartz, C. & Boudreau, R. (2006). Geotechnical Aspects of Pavements, FHWA NHI-05-037. Federal Highway Administration, U.S. Department of Transportation.

Donrak, J., Rachan, R., Horpibulsuk, S., Arulrajah, A. & Du, Y.J. (2016). Improvement of marginal lateritic soil using Melamine Debris replacement for sustainable engineering fill materials. Journal of Cleaner Production, **134**, B, 515-522.

Duskov, M. (1997). Materials Research on EPS20 and EPS15 Under Representative Conditions in Pavement Structures. Geotextiles and Geomembranes, **15**, No. 1-3, 147-181.

Duskov, M. (1997). Measurements on a Flexible Pavement Structure with an EPS Geofoam Sub-Base. Geotextiles and Geomembrane, **15**, No. 1-3, 5-27.

Duškov, M., den Uil, M. and Fütterer, M. (2019). Dutch A76 Highway Widening Using EPS Embankment with a Vertical Side. In: Arellano D., Özer A., Bartlett S., Vaslestad J. (eds). 5th International Conference on Geofoam Blocks in Construction Applications (pp. 81-87). Springer, Cham.

Expanded Polystyrene Used in Road Embankments - Design, Construction and Quality Assurance (1992). Form 482E. Oslo: Public Roads Administration, Road Research Laboratory.

Farnsworth, C.B., Bartlett, S.F., Negussey, D. & Stuedlein, A.W. (2008). Rapid Construction and Settlement Behavior of Embankment Systems on Soft Foundation Soils. Journal of Geotechnical and Geoenvironmental Engineering, **134**, No.3, 289-301.

Gandahl, R. (1987). Polystyrene Foam as a Frost Protection Measure on National Roads in Sweden, Transportation Research Record No. 1146. Washington, D.C.: Transportation Research Board.

Gao, H., Bua, C., Wang, Z., Shena, Y. & Chen, G. (2017). Dynamic characteristics of expanded polystyrene composite soil under traffic loadings considering initial consolidation state. Soil Dynamics and Earthquake Engineering, **102**, 86-98.

Gao, H., Hu, Y., Wang, Z., Wang, C. & Chen, G. (2017). Shaking table tests on the seismic performance of a flexible wall retaining EPS composite soil. Bull Earthquake Eng, **15**, No. 12, 5481–5510.

Georgees, R. N., Hassan, R. A., Evans, R. P., & Jegatheesan, P. (2018). An evaluation of performance-related properties for granular pavement materials using a polyacrylamide additive. International Journal of Pavement Engineering, **19**, No. 2, 153-163.

Gnanendran, C. T., Piratheepan, J., Ramanujam, J., & Arulrajah, A. (2011). Accelerated Laboratory Pavement Model Test on Cemented Base and Clay Subgrade. Geotechnical Testing Journal, 34, No. 4, 297-309.

Gonzalez-Torre, I., Calzada-Perez, M.A., Vega-Zamanillo, A. & Castro-Fresno, D. (2015). Evaluation of reflective cracking in pavements using a new procedure that combine loads with different frequencies. Construction and Building Materials, **75**, 368-374.

Horvath, J.S. (1994). Expanded Polystyrene (EPS) Geofoam: An Introduction to Material Behavior. Geotextiles and Geomembranes, **13**, No. 4, 263-280.

Horvath, J.S. (2010). Emerging Trends in Failures Involving EPS-Block Geofoam Fills. Journal of Performance of Constructed Facilities, 24, **No**. 4, 365-372.

Huang, Y.H. (1993). Pavement analysis and design. Englewood Cliffs, NJ: Prentice Hall, cop.,http://worldcat.org/isbn/0136552757.

Izevbekhai, B. I., & Pederson, N. (2011). Investigation of deflection and vibration dynamics of concrete and bituminous pavements constructed over geofoam. Minnesota Department of Transportation, Research Services Section.

Jegatheesan, P. & Gnanendran, C.T. (2016). Permanent Deformation Study of Pavement Layers Using Laboratory Pavement Model Testing. International Journal of Geomechanics, **16**, No. 3.

Keller, G.R. (2016). Application of geosynthetics on low-volume roads. Transportation Geotechnics, **8**, 119-131.

Kim, H., Choi, B. & Kim, J. (2010). Reduction of Earth Pressure on Buried Pipes by EPS Geofoam Inclusions. Geotechnical Testing Journal, **33**, No. 4, 304-313.

Lal B.R.R., Padade, A.H. & Mandal, J.N. (2014). Numerical Simulation of EPS Geofoam as Compressible Inclusions in Fly Ash Backfill Retaining Walls. Geo-Shanghai 2014. Shanghai, China.

Leshchinsky, B. & Ling, H.I. (2013). Numerical modeling of behavior of railway ballasted structure with geocell confinement. Geotextiles and Geomembranes, **36**, 33-43.

Lingwall, B.N. (2011). Development of an expanded polystyrene geofoam cover system for pipelines at fault crossing. PhD dissertation, The University of Utah, Department of Civil and Environmental Engineering.

Meguid, M.A., Ahmed, M.R., Hussein, M.G. & Omeman, Z. (2017). Earth Pressure Distribution on a Rigid Box Covered with U-Shaped Geofoam Wrap. International Journal of Geosynthetics and Ground Engineering.

Meguid, M.A., Hussein, M.G., Ahmed, M.R., Omeman, Z. & Whalenm, J. (2017). Investigation of soil-geosynthetic-structure interaction associated with induced trench installation. Geotextiles and Geomembranes, 45, No. 4, 320-330.

Moghaddas Tafreshi, S.N. & Dawson, A.R. (2010). Comparison of bearing capacity of a strip footing supported on sand reinforced with 3D and with planar geotextile. Geotextiles and Geomembranes, **28,** No. 1, 72-84.

Moghaddas Tafreshi, S.N., Khalaj, O. & Dawson, A.R. (2013). Pilot-scale load tests of a combined multilayered geocell and rubber-reinforced foundation. Geosynthetics International, **20**, No. 3, 143-161.

Mohajerani, A., Ashdown, M., Abdihashi, L. & Nazem, M. (2017). Expanded polystyrene geofoam in pavement construction. Construction and Building Materials, **157**, 438–448.

Negussey, D. (2007). Design Parameters for EPS Geofoam. Soils and Foundations, **47**, No. 1, 161-170.

Newman, M.P., Bartlett, S.F. & Lawton, E.C. (2010). Numerical Modeling of Geofoam Embankments. J. Geotech. Geoenviron. Eng., **136**, 290-298.

Ossa, A. & Romo, M.P. (2009). Micro- and macro-mechanical study of compressive behavior of expanded polystyrene geofoam. Geosynthetics International, **16**, No. 5, 327-338.

Ossa, A. & Romo, M.P. (2011). Dynamic characterization of EPS geofoam. Geotextiles and Geomembrane, **29**, No. 1, 40-50.

Özer, A.T. & Akınay, E. (2019). First Geofoam Roadway Embankment Application in Turkey. In: Arellano D., Özer A., Bartlett S., Vaslestad J. (eds). 5th International Conference on Geofoam Blocks in Construction Applications (pp. 71-80). Springer, Cham.

Ozer, A.T. (2016). Laboratory study on the use of EPS-block geofoam for embankment widening. Geosynthetics International, **23**, No. 2, 71-85.

Palmeira, E.M. & Antunes, L.G.S. (2010). Large scale tests on geosynthetic reinforced unpaved roads subjected to surface maintenance. Geotextiles and Geomembranes, **28**, No. 6, 547-558.

Piratheepan, J., Gnanendran, C.T. & Arulrajah, A. (2012). Determination of c and φ from IDT and Unconfined Compression Testing and Numerical Analysis. Journal of materials in civil engineering, 24, No. 9.

Powell, W.D., Potter, J.F., Mayhew, H.C. & Nunn, M.E. (1984). The structural design of bituminous roads, TRRL Report LR 1132, Crowthorne, UK.

Pu, X., Shi, Z. & Xiang, H. (2018). Feasibility of ambient vibration screening by periodic geofoam-filled trenches. Soil Dynamics and Earthquake Engineering, **104**, 228–235.

Qiu, Y., Dennis, N.D. & Elliott, R.P. (2000). Design Criteria for Permanent Deformation of Subgrade Soils in Flexible Pavements for Low-Volume Roads. Soils and Foundations, **40**, No. 1, 1-10.

Rahman, M. A., Imteaz, M. A., Arulrajah, A., Piratheepan., J. & Disfani, M. M. (2015). Recycled construction and demolition materials in permeable pavement systems: geotechnical and hydraulic characteristics. Journal of Cleaner Production, **90**, 183-194.

Shafikhani A., Bheemasetti T.V., Puppala A.J. & Banerjee A. (2018). Analysis and Interpretation of Inclinometer and Pressure Cell Data on a Soil-Geofoam Embankment. In: Hu L., Gu X., Tao J., Zhou A. (eds). Proceedings of GeoShanghai 2018 International Conference: Multi-physics Processes in Soil Mechanics and Advances in Geotechnical Testing. GSIC 2018. Springer, Singapore.

Shafikhani, A., Bheemasetti, T.V. & Puppala, A.J. (2017). Effect of Seasonal Changes on a Hybrid Soil–Geofoam Embankment. International Journal of Geosynthetics and Ground Engineering.

Stark, T.D. (2004). NCHRP Report 529: Guideline and Recommended Standard for Geofoam Applications in Highway Embankments. Transportation Research Board, Washington, D.C.

Stark, T.D., Arellano, D., Horvath, J.S. & Leshchinsky, D. (2004). NCHRP Web Document 65 (Project 24-11): Geofoam Applications in the Design and Construction of Highway Embankments. Transportation Research Board, Washington, D.C.

Stark, T.D., Bartlett, S.F. & Arellano, D. (2012). Expanded Polystyrene (EPS) Geofoam Applications and Technical Data. The EPS Industry Alliance.

Tanyu, B.F., Aydilek, A.H., Lau, A.W., Edil, T.B. & Benson, C.H. (2013). Laboratory evaluation of geocell-reinforced gravel subbase over poor subgrades. Geosynthetics International, **20**, No. 2, 47-61.

Tavira, J., Jiménez, J.R., Ayuso, J., Sierra, M.J. & Ledesma, E.F. (2018). Functional and structural parameters of a paved road section constructed with mixed recycled aggregates from non-selected construction and demolition waste with excavation soil. Construction and Building Materials, **164**, 57-69.

Thakur, J.K., Han, J., Pokharel, S.K. & Parsons, R.L. (2012). Performance of geocell-reinforced recycled asphalt pavement (RAP) bases over weak subgrade under cyclic plate loading. Geotextiles and Geomembranes **35**, 14-24.

Trandafir, A.C. & Erickson, B.A. (2012). Stiffness Degradation and Yielding of EPS Geofoam under Cyclic Loading. Journal of Materials in Civil Engineerin, **24**, No. 1.

Trandafir, A.C., Bartlett, S.F. & Lingwall, B.N. (2010). Behavior of EPS geofoam in stress-controlled cyclic uniaxial tests. Geotextiles and Geomembranes, **28**, No. 6, 514-524.

Uzan, J. (1985). Characterization of Granular Material. Transportation Research Record No. 1022, 52-59.

Vaslestad, J., Liveroed J.E., Damtew T., Singstad S. & Loevstad D. (2019). Geofoam Eps Used in Bridge Abutment, E18 Farris Bridge. In: Arellano D., Özer A., Bartlett S., Vaslestad J. (eds). 5th International Conference on Geofoam Blocks in Construction Applications (pp. 49-55). Springer, Cham.

Witthoeft, A.F. & Kim, H. (2016). Numerical investigation of earth pressure reduction on buried pipes using EPS geofoam compressible inclusions. Geosynthetics International, **23**, No. 4, 287-300.

Wong, H. & Leo, C.J. (2006). A simple elastoplastic hardening constitutive model for EPS geofoam. Geotextiles and Geomembranes, **24**, No. 5, 299-310.

Yang, X., Han, J., Pokharel, S.K., Manandhar, C., Parsons, R.L., Leshchinsky, D. & Halahmi, I. (2012). Accelerated pavement testing of unpaved roads with geocell-reinforced sand bases. Geotextiles and Geomembranes, **32**, 95-103.

Zou, Y., Small, J.C. & Leo, C.J. (2000). Behavior of EPS Geofoam as Flexible Pavement Subgrade Material in Model Tests. Geosynthetics International, **7**, No. 1, 1-22.

List of Tables

List of Figures

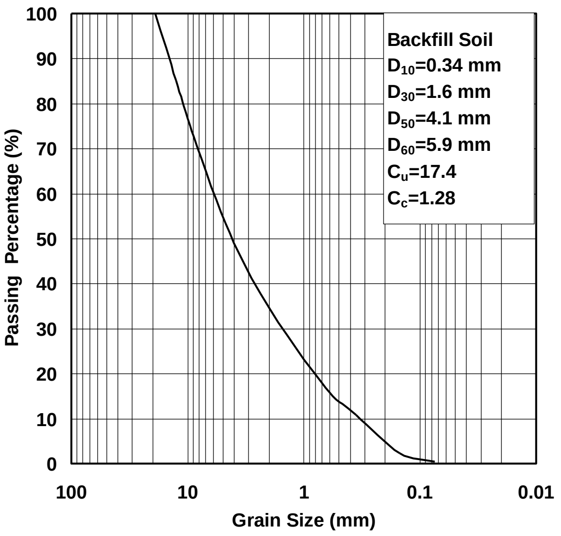

Fig. 1 Grain size distribution curves for backfill soil (ASTM D 2487)

1077
1078

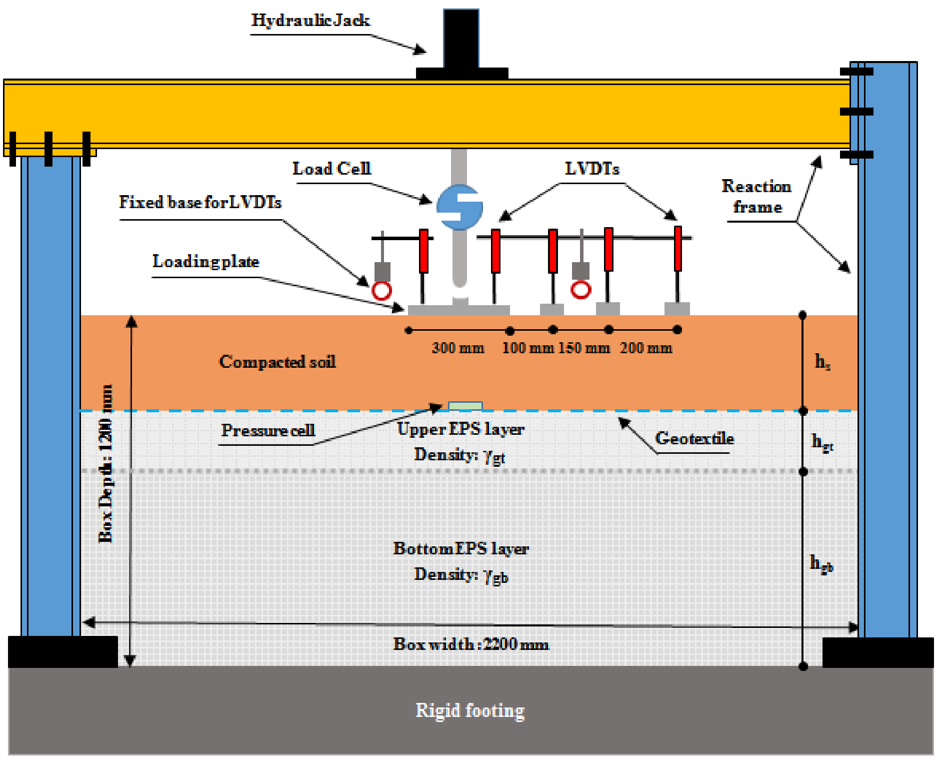

Fig. 2. Schematic view of the testing apparatus (not to scale) and test parameters.

1079

(a) **(b)**

Fig. 3. (a) Placement of EPS geofoam blocks inside test box and, (b) Completed test installation prior to loading including reaction beam, loading plate, hydraulic jack, load cell and LVDTs

1080

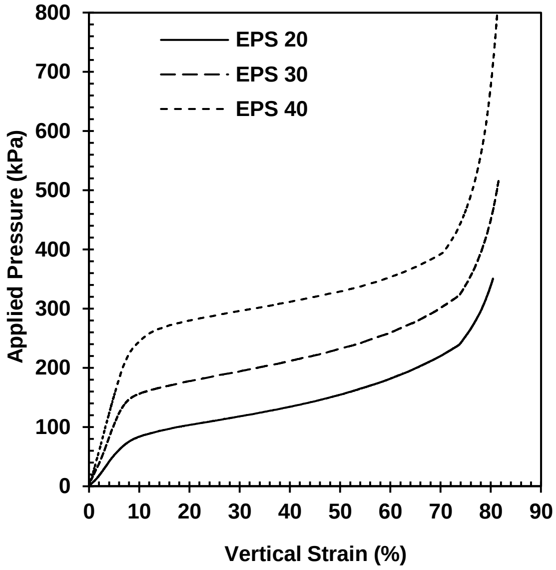

Fig. 4. Stress-strain diagram for static loading on EPS with densities 20, 30 and 40 kg/m^3.

1081
1082

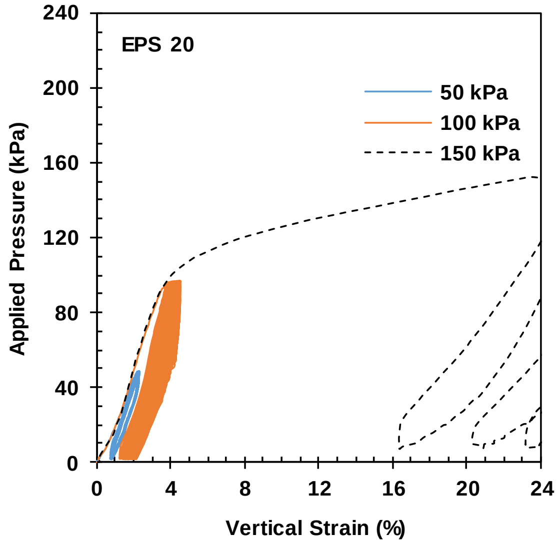

(a)

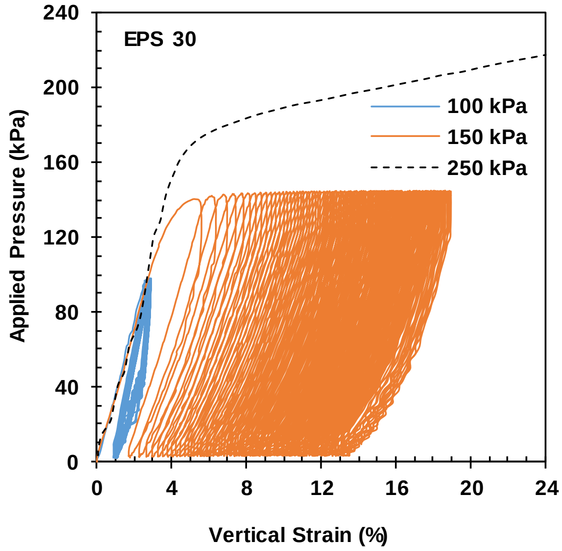

(b)

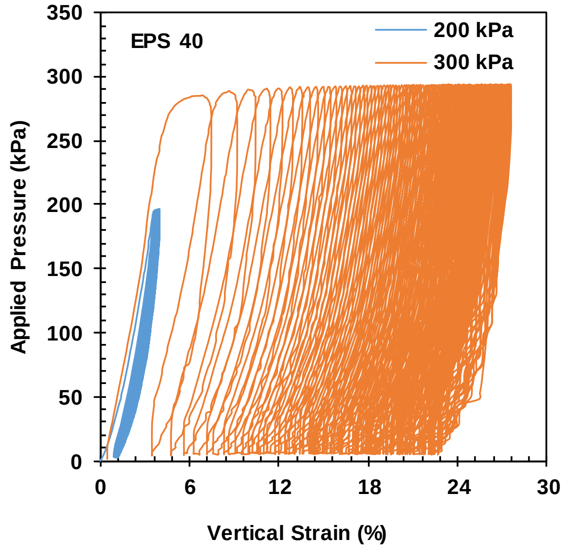

(c)

Fig. 5. Hysteresis response of EPS cubic geofoam sample for (a) EPS 20, (b) EPS 30 and (c) EPS 40

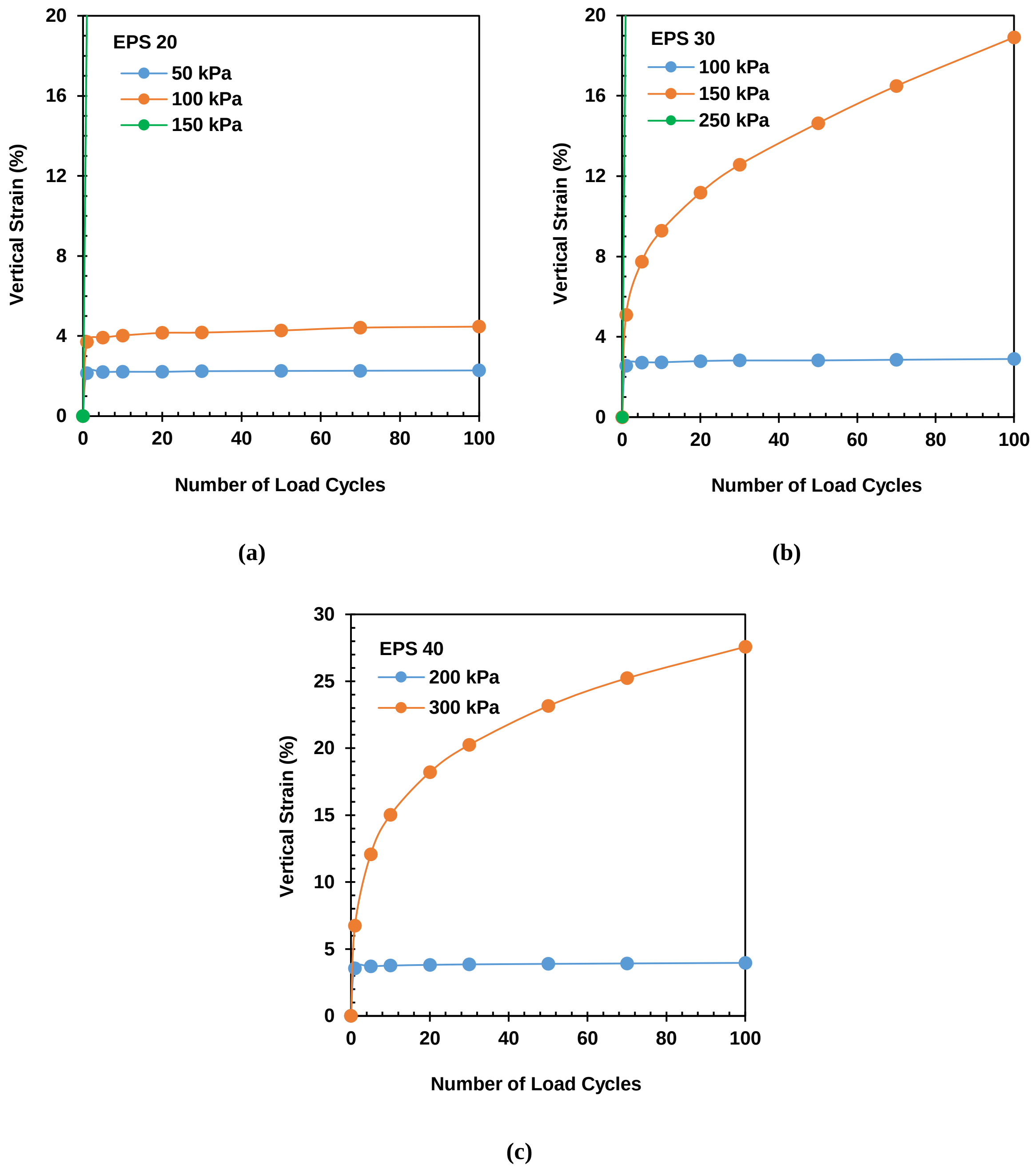

Fig. 6. Variation of peak vertical strain against the number of load cycle for (a) EPS 20, (b) EPS 30 and (c) EPS 40

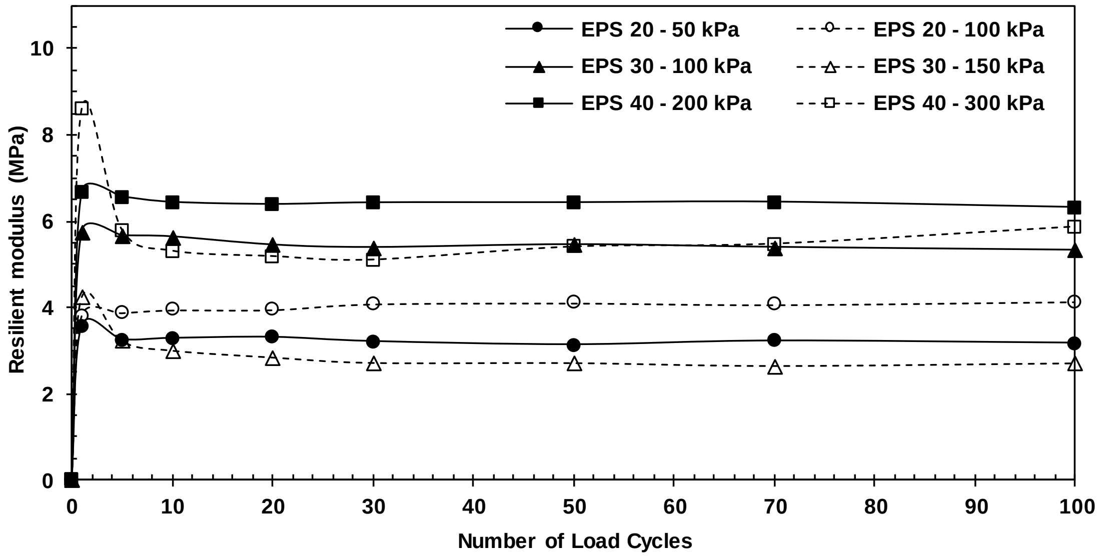

Fig. 7. Resilient modulus of EPS 20, EPS 30 and EPS 40 under two different amplitudes of applied pressure for each density.

1087

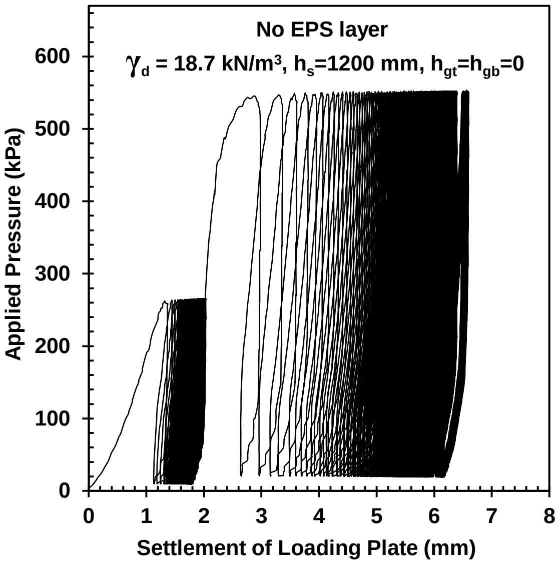

(a)

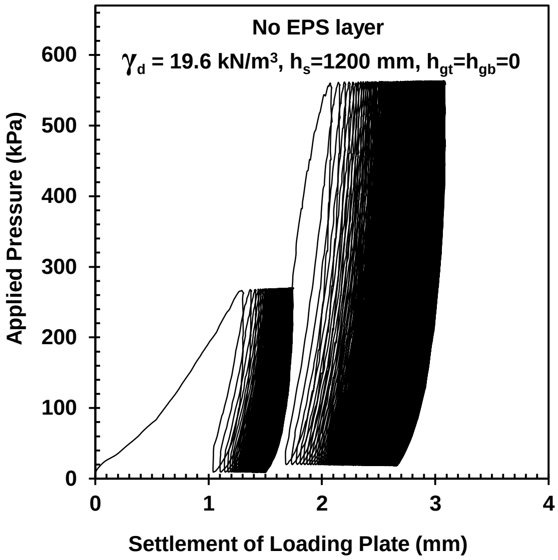

(b)

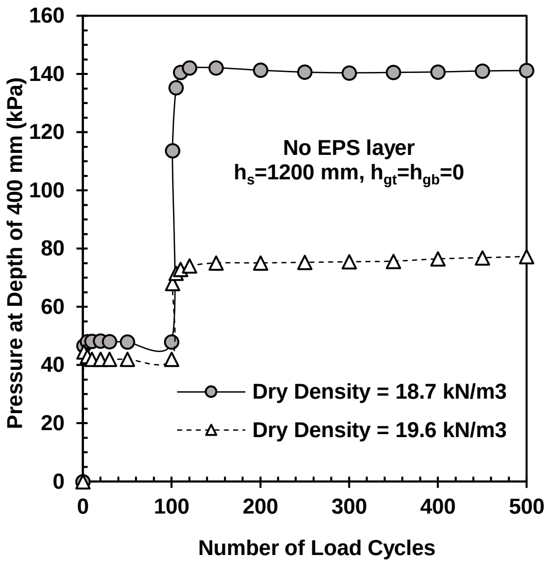

(c)

Fig. 8. Settlement of pressure surface under 100 cycles of 275 kPa and 400 cycles of 550 kPa for (a) soil dry density of 18.7 kN/m^3, (b) soil dry density of 19.6 kN/m^3 and (c) Variation soil pressure with number of load cycles at depth of 400 mm.

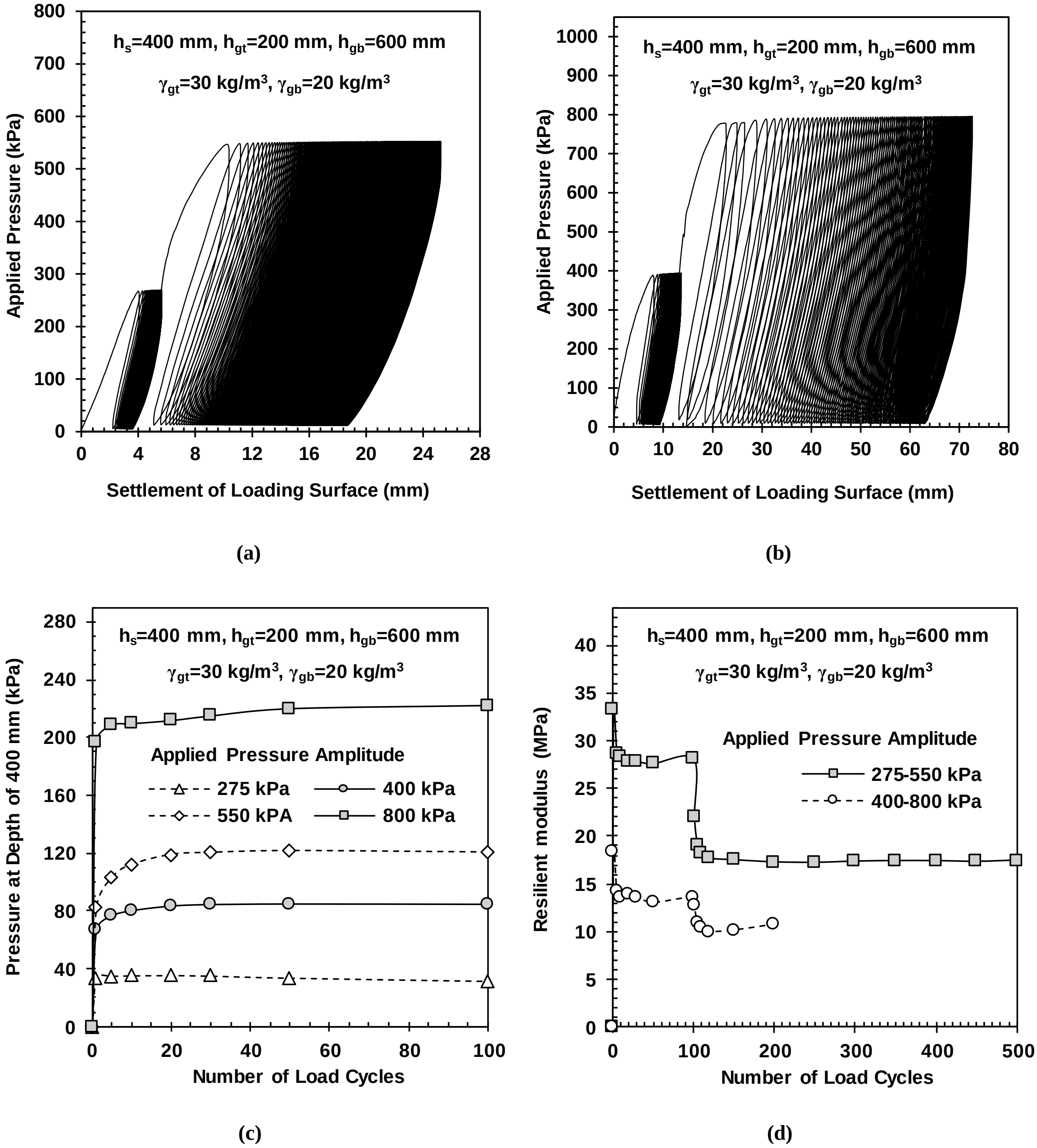

Fig. 9. Settlement of loading surface for different pressures of cyclic loading (a) after 500 cycles of reduced loading (paved road), (b) after 200 cycles of original loading (unpaved road) and (c) Measured pressure at depth of 400 mm during the first 100 cycles of each loading intensity (d) Resilient modulus of pavement for each loading intensity scenarios.

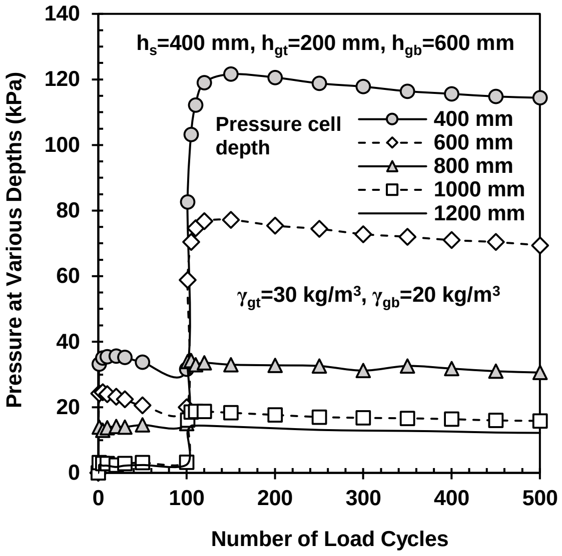

Fig. 10. Measured pressure at different layers of EPS geofoam for 100 cycles of 275 kPa and 400 cycles of 550 kPa pressures.

1092

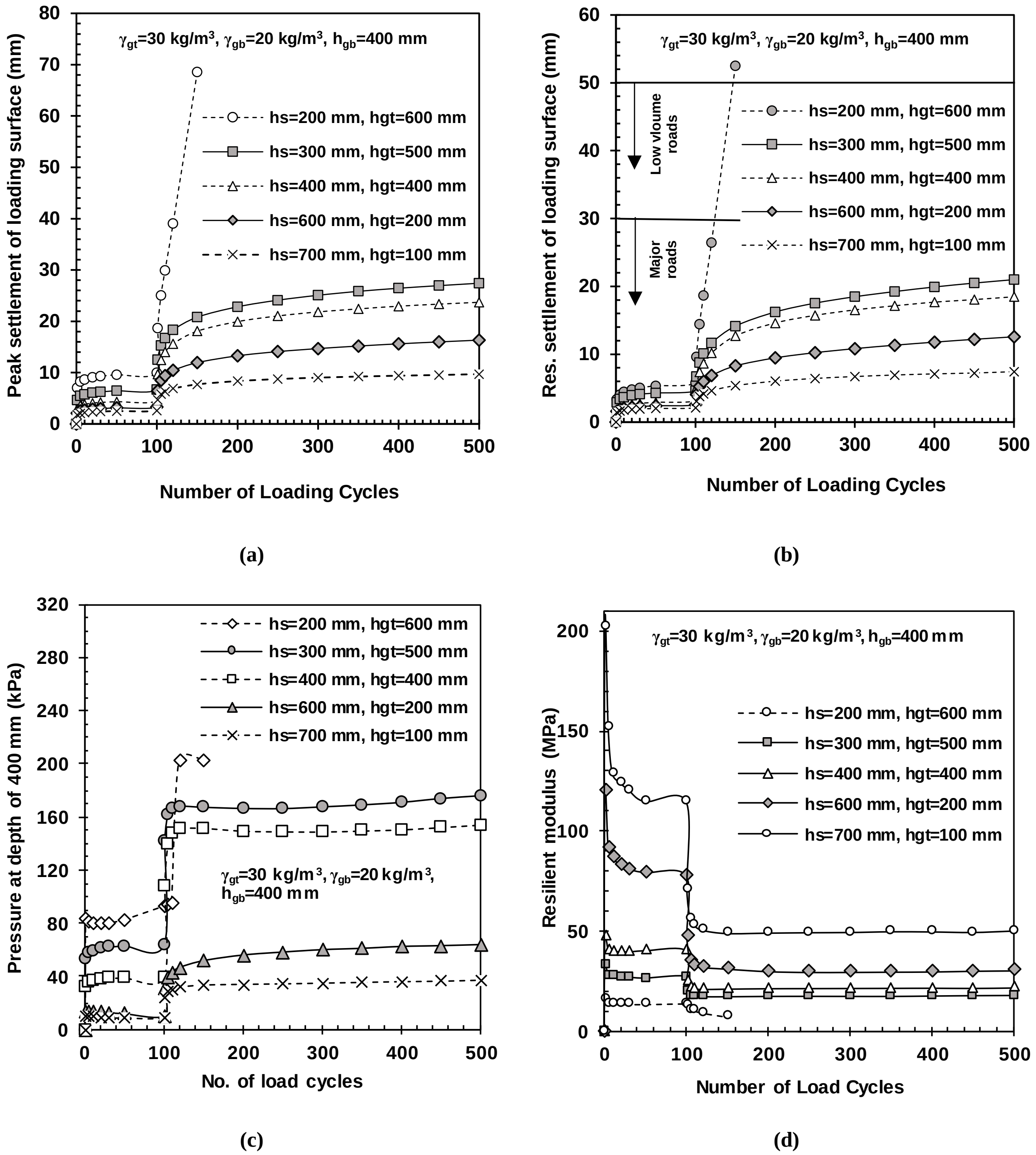

Fig. 11. Variation of (a) total settlements and (b) residual settlements versus number of loading cycles for different values of soil and upper EPS layer thickness (h_s and h_{gt}) and, (c) Variation of transferred pressure at depth of 400 mm (top of EPS 30) for different values of h_s and h_{gt}, (d) Resilient modulus of pavements with different soil and upper EPS layers' thicknesses.

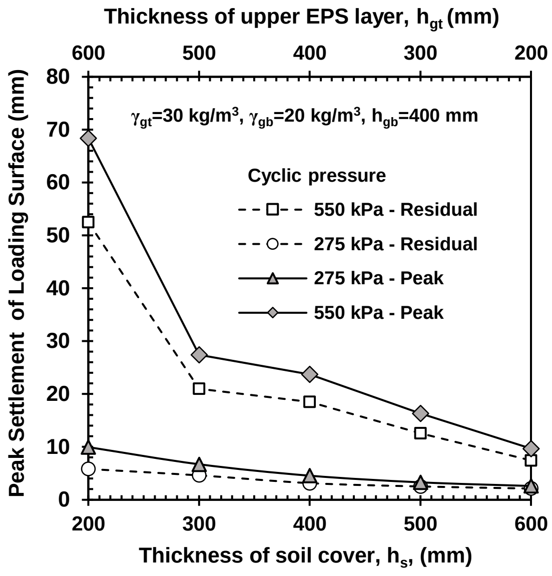

Fig. 12. Variation of the maximum values of peak and residual settlement for different thicknesses of soil and upper EPS layers (h_s and h_{gt}).

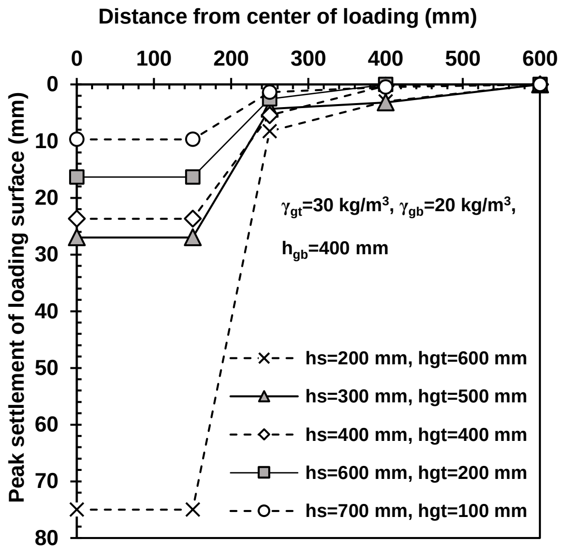

Fig. 13. Profile of the peak settlements for different values of h_s and h_{gt}.

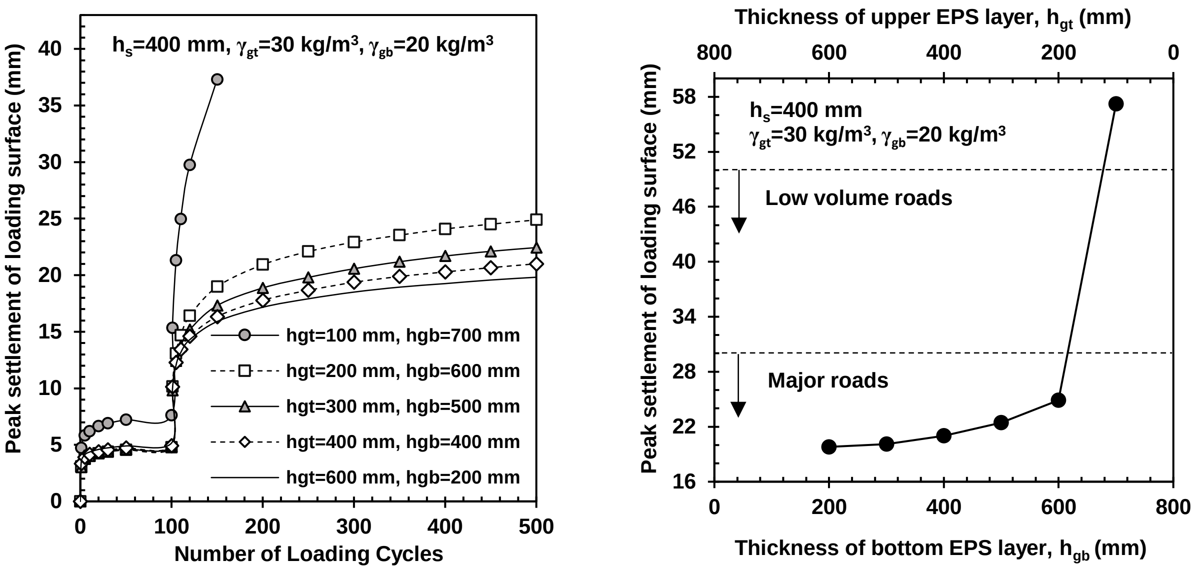

(a) **(b)**

Fig. 14. (a) Settlement of loading surface with respect to no. of load cycles for different values of h_{gt} and h_{gb}, (b) Peak value of surface settlements for different values of h_{gt} and h_{gb}.

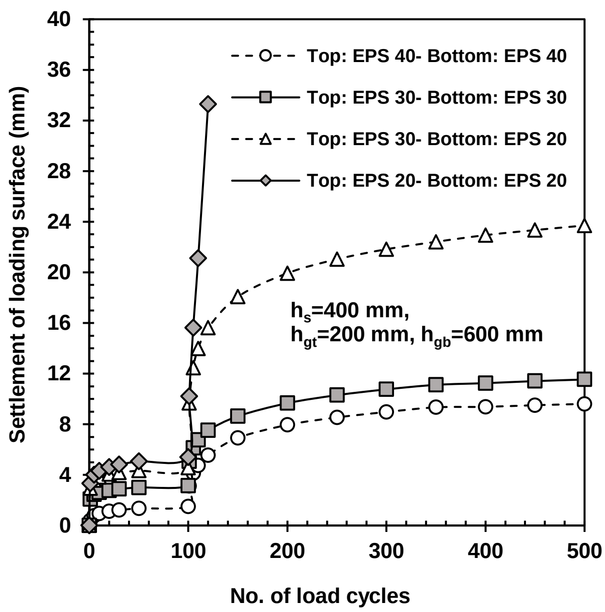

Fig. 15. Settlement of loading surface with respect to no. of loading cycles for different values of EPS density at top and bottom layers

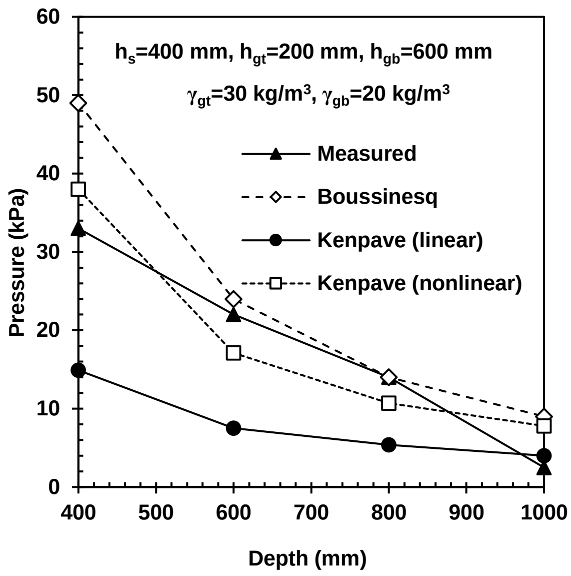

Fig. 16. Transferred pressure at different depths obtained from analytical methods and test measurements for applied pressure of 275 kPa

1104

1105

1106

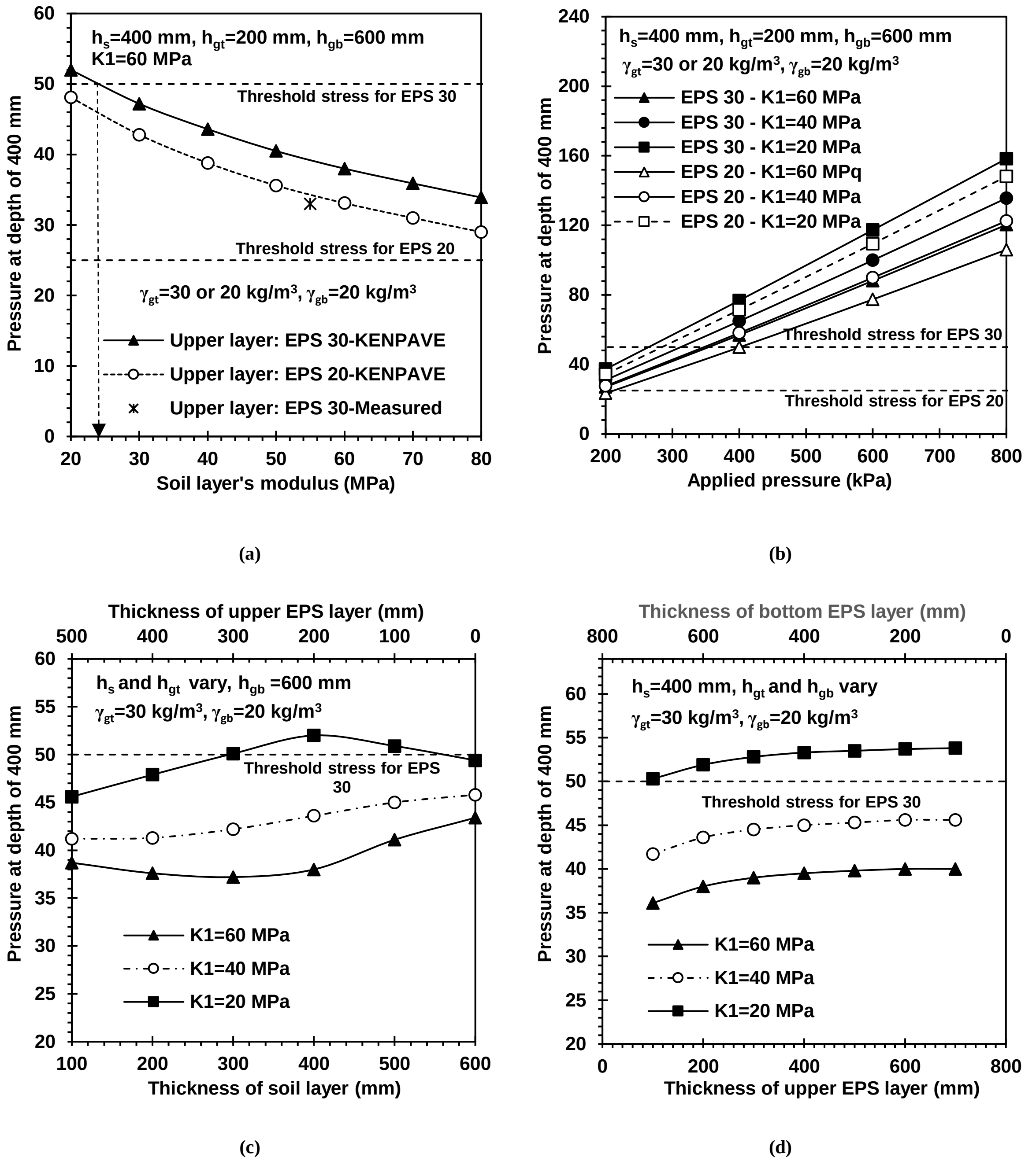

Fig. 17. (a) Variation of transferred pressure on the top of upper EPS layers for different moduli of soil layer compared to the measured value for applied pressure of 275 kPa for the pavement with EPS 30 or EPS 20 as the top layer, (b) Effect of applied pressure intensity on the transferred pressure over the upper EPS layer, (c) Effect of soil and upper EPS layer thickness on the transferred pressure on the upper EPS layer and (d) Effect of upper and bottom EPS layer thicknesses on the transferred pressure on the upper EPS layer

Table 1. Summary of research on EPS geofoam subgrades

Overview of Research Title	Researcher Name	Main Objectives/Remarks	Suggestions for Development/ Possible Shortcomings	Year
EPS geofoam in pavement construction	Mohajerani et al.	A review of design considerations and application of EPS in roads	No specific study on the described issues	2017
Application of geosynthetics (including EPS) in roads	Keller	A brief overview on several types of Geosynthetics for low volume roads	No detailed discussion on EPS geofoam	2016
Geocell-reinforced subbase over poor subgrades (EPS geofoam as poor subgrade)	Tanyu et al.	Determine performance of Geocell over poor subgrades	No evaluation on the performance of EPS geofoam	2013
Effectiveness of connectors in EPS block construction	Barrett and Valsangkar	Study a few methods of EPS block connection	No evaluation on the performance of EPS geofoam per se	2009
Rapid construction of embankment using EPS block	Farnsworth et al.	Comparison of several techniques for construction on soft soils	No detailed discussion on EPS geofoam	2008
Design parameters for EPS geofoam	Negussey	Modify Design Parameters for EPS	No evaluation of the effect of soil thickness, EPS geofoam density or its thickness	2007
EPS geofoam as flexible pavement subgrade material	Zou et al.	Study performance of EPS subgrades	No evaluation of the effect of soil thickness, EPS geofoam density or its thickness	2000
Flexible pavement structure with an EPS geofoam sub-base	Duskov	Measurement of EPS pavement performance under heavy traffic loading	No evaluation of the effect of soil thickness, EPS geofoam density or its thickness	1997

Table 2. Physical and mechanical properties of EPS geofoam

Engineering properties	Values for EPS 20	Values for EPS 30
Real density (kg/m^3)	17~19	27~29
Angle of internal friction (º)	~ 2	~ 3
Apparent cohesion (kPa)	~40	~70
Elastic modulus (MPa)	0.81	2.16
Compressive Strength (kPa)	83.67	156.4

Table 3. The engineering characteristics of geotextile

Property	**Value**
Type of geotextile	Non-woven
Material	Polypropylene
Mass per unit area (gr/m^2)	170
Tensile strength (MD), kN/m	16
Tensile strength (CMD), kN/m	18
Elongation at maximum load, %	>50
Static puncture (CBR), kN	2.7

Table 4. Test program for large cyclic plate load experiments

<table>
<tr><th>Test Series</th><th>h_s (mm)</th><th>h_{gt} (mm)</th><th>h_{gb} (mm)</th><th>γ_{gt} (kg/m^3)</th><th>γ_{gb} (kg/m^3)</th><th>Soil density (kN/m^3)</th><th>Cyclic pressure (kPa)</th><th>No. of Tests</th><th>Purpose of the Test</th></tr>
<tr><td>1</td><td>1200</td><td>-</td><td>-</td><td>-</td><td>-</td><td>18.7, 19.6</td><td>275-550</td><td>2+3*</td><td>To evaluate behavior of soil backfill</td></tr>
<tr><td>2</td><td>400</td><td>200</td><td>600</td><td>30</td><td>20</td><td>18.7 to 19.6**</td><td>400-800</td><td>1+2*</td><td>To determine the effect of applied pressure amplitude</td></tr>
<tr><td>3</td><td>400</td><td>200</td><td>600</td><td>30</td><td>20</td><td>18.7 to 19.6**</td><td>275-550</td><td>5*** +4*</td><td>To determine the stress distribution in depth of EPS geofoam</td></tr>
<tr><td rowspan="4">4</td><td>200</td><td>600</td><td rowspan="4">400</td><td rowspan="4">30</td><td rowspan="4">20</td><td rowspan="4">18.7 to 19.6**</td><td rowspan="4">275-550</td><td rowspan="4">4+5*</td><td rowspan="4">To evaluate the combined effect of soil and upper EPS layers thickness</td></tr>
<tr><td>300</td><td>500</td></tr>
<tr><td>600</td><td>200</td></tr>
<tr><td>700</td><td>100</td></tr>
<tr><td rowspan="4">5</td><td rowspan="4">400</td><td>100</td><td>700</td><td rowspan="4">30</td><td rowspan="4">20</td><td rowspan="4">18.7 to 19.6**</td><td rowspan="4">275-550</td><td rowspan="4">4+4*</td><td rowspan="4">To recognize the combined effect of upper and bottom EPS layers thickness</td></tr>
<tr><td>300</td><td>500</td></tr>
<tr><td>400</td><td>400</td></tr>
<tr><td>600</td><td>200</td></tr>
<tr><td rowspan="3">6</td><td rowspan="3">400</td><td rowspan="3">200</td><td rowspan="3">600</td><td>40</td><td>40</td><td rowspan="3">18.7 to 19.6**</td><td rowspan="3">275-550</td><td rowspan="3">3+2*</td><td rowspan="3">To specify the influence of EPS density</td></tr>
<tr><td>30</td><td>30</td></tr>
<tr><td>20</td><td>20</td></tr>
</table>

** Indicates the number of tests which have been repeated two or three times to ensure the accuracy of the test data. For example, in test Series 6, a total of 5 tests were performed, including 3 independent tests plus 2 replicates.*

*** Density of soil layers vary from 18.7 to 19.6 (kN/m3) from bottom to top of soil cover*

**** Due to insufficient number of available pressure cells, one test was repeated 5 times with placing the pressure sensor at the indicated depths (400, 600, 800, 1000 and 1200 mm below the loading surface in separate tests)*

Table 5- Calibration factors for nonlinear analysis

Material	**Calibration factors**	
	K1 (kPa)	**K2**
Soil	60,000	-0.25
Upper EPS (EPS 30)	10,000	-0.01
Bottom EPS (EPS 20)	6,000	-0.01

Table 6- Comparison of linear and nonlinear methods with those of test measurements for applied pressure of 275 kPa

Method	Surface settlement (mm)	Measured/calculated pressures (kPa) at depths			
		400 (mm)	600 (mm)	800 (mm)	1000 (mm)
Test measurement	4	33	22	14	2.5
Boussinesq	-	49	24	14	9
KENPAVE (linear)	2.5	14.9	7.5	5.4	4
KENPAVE (nonlinear)	3.8	38	17.1	10.7	7.8